FAST CAPILLARY CHROMATOGRAPHY AND IMMUNOAFFINITY CHROMATOGRAPHY COUPLED WITH CAPILLARY ZONE ELECTROPHORESIS

By

LAURA JANE COLE

A DISSERTATION PRESENTED TO THE GRADUATE SCHOOL
OF THE UNIVERSITY OF FLORIDA IN PARTIAL FULFILLMENT
OF THE REQUIREMENTS FOR THE DEGREE OF
DOCTOR OF PHILOSOPHY

UNIVERSITY OF FLORIDA

1995

To my husband Scott.

ACKNOWLEDGMENTS

I would like to thank my advisor, Bob Kennedy for his support during my stay at the University of Florida. I would like to thank the members of the Kennedy group for their help and advice during my time spent at the University of Florida. I would like to thank Nicole Schultz and Monica Escobar for advice and support during my graduate school career.

TABLE OF CONTENTS

Abstract of Dissertation Presented to the Graduate School
of the University of Florida in Partial Fulfillment of the
Requirements for the Degree of Doctor of Philosophy

FAST CAPILLARY CHROMATOGRAPHY AND IMMUNOAFFINITY CHROMATOGRAPHY COUPLED WITH CAPILLARY ZONE ELECTROPHORESIS

By

Laura Jane Cole

May 1995

Chairman: Robert T. Kennedy
Major Department: Chemistry

Column designs that allow rapid separation by packed capillary liquid chromatography were explored. A two column separation system using immunoaffinity chromatography and capillary electrophoresis was developed. The chromatography column was used as a selective preconcentrator for capillary zone electrophoresis (CZE). This two column system was also used for epitope mapping.

Rapid separations were obtained using capillaries packed with pellicular and perfused particles. These columns were evaluated by using a nominally unretained solute to determine plate height as a function of flow velocity in capillaries from 50 to 250 μm inner diameter (i.d.). A decrease in both column i.d. and column i.d. to particle diameter ratio(ρ) were found to improve the performance of columns packed with pellicular

particles. The most important factor was ρ. The best results were obtained with a 50 μm i.d. column packed with 8 μm glass beads. In 10 s these columns generated nearly 7,000 theoretical plates.

Immunoaffinity columns were tested with protein G and epoxide activated perfused particles. Protein G columns were used to selectively preconcentrate insulin onto a CZE system. Experiments were performed off-line in which fractions were collected from the immunoaffinity column and then injected onto the CZE. On-line experiments were also performed in which a flow-gated interface was used to couple the two columns directly. Flow rates as high as 100 μL/min were used to load sample onto the affinity column. A desorbing flow rate of less than 10 μL/min was used to limit dilution effects to the analyte. Preconcentration up to 1000-fold was obtained.

Immunoaffinity columns were also used to bind peptide fragments resulting from digestion of glucagon like peptide-1 7-36. CZE and matrix assisted laser desorption ionization time of flight mass spectrometry were used to characterize whole digests, bound portion of the digests and unbound portion of the digests. The determination of linear epitopes can be performed using these methods. The epitope region for glucagon like peptide -1 7-36 was narrowed down to the first six peptides using this method.

CHAPTER 1
INTRODUCTION

Microcolumn separations have been used recently to improve separation efficiency and enable small samples to be used (1-4). One purpose of the work described in this dissertation is to develop column designs which give fast and highly efficient separations in packed capillary liquid chromatography. Capillary columns of inner diameters (i.d.) from 50-250 μm were packed with two types of particles. The types of particles which were used in the work presented in this dissertation are used to decrease band broadening. Therefore, capillary columns packed with these particles should allow fast separations.

The second part of this dissertation will explore the use of immunoaffinity chromatography coupled with capillary zone electrophoresis (CZE). One application which is explored is using the affinity column as a selective preconcentrator for CZE. Another application which is investigated is epitope mapping using the affinity column to bind peptide fragments corresponding to the epitope region of the antigen used. Epitope mapping is the process of determining the specific region of an antigen that an antibody recognizes. CZE and matrix assisted laser desorption ionization time of flight mass spectrometry (MALDI-TOFMS) are then used to compare digestion products, bound fragments and unbound fragments from the digestion of the antigen.

Capillary Liquid Chromatography

Capillary liquid chromatography (LC) has significant advantages over conventional liquid chromatography. These advantages include higher column efficiencies, low volumetric flow rates, and small sample size compatibility (5). The low volumetric flow rates used in capillary chromatography are compatible to interfacing with a mass spectrometry system. Another consideration is that by using a lower flow rate less waste is generated, and also a smaller volume of solvents are used. Therefore, if exotic or expensive solvents are used, their consumption can be reduced. With their small sample size requirement, capillary LC separations are ideal for cases where only a small amount of sample is available, such as from biological systems.

There are three main types of capillary liquid chromatography: open tubular, partially packed, and fully packed capillaries (see Figure 1-1) (5). Open tubular capillaries have i.d.s between 3 and 50 μm and are coated with a thin film of stationary phase. Although open tubular capillaries offer very high efficiencies, there are several disadvantages to their use. First, they have a low surface area which limits the capacity of the column. Open tubular capillaries can be difficult to prepare as the small diameter capillaries are easily clogged. Byproducts from the stationary phase procedure can also be difficult to remove from the small capillaries. Finally, reproducibility and stability are poor due to the solvent eroding the stationary phase.

Partially packed capillaries have been explored as a possible type of capillary LC (6). A narrow bore glass tube which has thick walls is packed tightly with particles and then the glass is drawn to the desired diameter with a glass drawing machine. As is shown in

Figure 1-1, the individual particles are embedded in the wall of the capillary. Upon development of this type of capillary it was hoped that partially packed capillaries would offer a good sample capacity with high efficiencies. However, they are difficult to prepare with good efficiency and are not in wide use.

Fully packed capillaries are used more extensively. Usual i.d.s are between 40 and 200 μm. One advantage to using packed capillaries are the many commercial packings available allowing preparation of columns suited to a variety of applications. Sample capacity for packed capillaries is higher than for open tubular or partially packed capillaries. Finally, although plate heights in packed capillaries are not as low as in open tubular columns, high numbers of theoretical plates can be achieved by increasing the length of the column (5).

There are three types of particles used in packed capillary chromatography. Figure 1-2 shows simple representations of the three types of particles. Porous particles are the most commonly used. Typical diameters are from 2 to 10 μm and pore sizes range from 60 to 4000 Å (7). The pores allow a high surface area, thereby increasing the capacity of the column. When the pores are relatively large, the mobile phase becomes stagnant in the pore. This stagnant mobile phase in the pores can lead to band broadening which decreases the efficiency of the separation. One type of particle which has been used to decrease this broadening term is a solid particle (8, 9). As there are no pores in the particle, there is not a stagnant mobile phase effect. However, there is a smaller sample capacity with solid particles as compared with porous particles. A third type of particle is a perfused particle (10). There are two types of pores in perfused particles: throughpores

and diffusive pores. The throughpore has a diameter of 6000 to 8000 Å which allows flow through the particle. The smaller, diffusive pore of 800 to 1500 Å diameter provides a greater surface area to the particle. In the research reported in this dissertation, pellicular (solid) and perfused particles were examined to determine the best column design for fast and efficient separations (11).

Dual Column Separation Methods

A powerful tool for the analysis of complex samples are dual column separation methods. It may not be possible for one separation method by itself to resolve all of the components in a complex sample. By injecting the partially resolved sample from the first column onto a second and different separation column, additional resolution can occur. When dual columns are used for one separation, the peak capacity for the separation is given by

$$n_s = n_1 \times n_2 \qquad \text{Equation 1-1}$$

where n_1 and n_2 are peak capacities for the individual separation methods (12). For this equation to be true, it is important for the separation methods to be based on different, unrelated properties.

There have been several types of dual column separation techniques explored. Bushey and Jorgenson have coupled a cation exchange column for the first column and then used a size exclusion column for the second column (13). Their method was used to separate a protein mixture and proteins from serum samples. All of the effluent from the first column was collected and then injected onto the second column. Another dual column method developed by Bushey and Jorgenson for the separation of peptides

involved a reversed phase column coupled with capillary zone electrophoresis (CZE) (14). The effluent of the chromatography column was sampled every minute by injecting onto the CZE although the whole sample volume from the chromatography column was not injected. Finally, a microcolumn size exclusion column has been coupled to CZE using a transverse flow gating interface (3). The gating interface allows a buffer to rinse column effluent to waste until a sample injection is desired, then the gating flow buffer is stopped and an injection performed onto the CZE column.

Dual column separation methods have also been developed using immunoaffinity chromatography coupled with a second separation column, usually a reversed phase liquid chromatography column (4, 15-17). A dual column immunoassay has been developed to avoid limitations of classical immunoaffinity chromatography. In classical immunoaffinity chromatography, the desorption kinetics of the dissociation of antigen-antibody complex can be slow, resulting in broad antigen peaks. Another problem arises from interference of the desorption buffer with the antigen peak. The desorption buffer can lead to large shifts in refractive index and in absorbance at the elution time. This can obscure the analyte peak. If a dual column immunoassay (DCIA) is used, these disadvantages can be removed. Regnier and co-workers have demonstrated a DCIA using a protein G affinity column coupled to a reversed phase column to determine antigen concentrations in complex samples (15). Several applications in which DCIA has been demonstrated are in the determination of multiple antigens (16), the cross-reactivities of antibodies (17), and human plasma proteins (4).

In order to inject sample from one column to another, several methods are employed. One method involves fraction collection of the effluent from the first column; this fraction can be collected off-line in a vial or on-line with the second separation technique. For on-line fraction collection, a switching valve is used to collect the area of interest from the first column and then reinject this directly onto the second column. This method relies on the knowledge of the elution time for the area of interest. A second method of on-line injection uses the effluent from the first column coupled directly with the second column, allowing all of the sample to be injected onto the second separation technique.

A schematic of a DCIA method which was used in the work presented in this dissertation is shown in Figure 1-3. Two applications of this dual column separation system were explored. The use of the immunoaffinity column as a preconcentrator for capillary zone electrophoresis was investigated (18). Another application of immunoaffinity chromatography coupled with CZE which was investigated was the determination of linear epitopes using an antigen/antibody pair with a known epitope region (19).

Capillary Zone Electrophoresis

The second separation technique in the dual column system explored was CZE which can allow high efficiency separations. Figure 1-4 shows a simple CZE setup. A 25-75 μm i.d. fused silica capillary is filled with a buffer solution. Sample is injected onto the column by hydrodynamic or electrokinetic methods. An electric field is applied across the capillary, thereby moving the sample through the capillary to the detector. By using small

diameter capillaries, joule heating is efficiently dissipated and there are negligible thermal and density gradients (20). Other modes of capillary electrophoresis include gel, isoelectric focusing and isotachophoresis.

The time it takes the analyte to migrate from the injection end of the capillary to the detector is given by

$$t_m = \frac{L^2}{(\mu + \mu_{osm})V} \qquad \text{Equation 1-2}$$

t_m is the migration time, L is the detection length, μ is the electrophoretic mobility of the analyte, μ_{osm} is the electroosmotic mobility and V is the voltage applied (20). A short capillary and high voltage applied will give short separation times. A measure of the efficiency of a separation can be described by the number of theoretical plates which are generated from a sample zone. This can be described by the following equation

$$N = \frac{(\mu + \mu_{osm})V}{2D} \qquad \text{Equation 1-3}$$

where D is the diffusion coefficient of the solute (20). Therefore, high efficiencies will result from high voltages applied.

The resolution of a separation is also an important consideration. If the resolution between two analytes is not high enough, the analytes will not be separated from each other. An equation for resolution is given below

$$R_s = \frac{N^{1/2}}{4} * \frac{\mu_1 - \mu_2}{\mu_{av} + \mu_{osm}} \qquad \text{Equation 1-4}$$

where μ_1 and μ_2 are the electrophoretic mobilities of the analytes and μ_{av} is the average of μ_1 and μ_2 (20). The best resolution occurs when the electroosmotic flow just balances the

average electrophoretic mobilities. An approximation for electrophoretic mobility is given by

$$\mu = \frac{z}{m^{2/3}} \qquad \text{Equation 1-5}$$

where z is the charge and m the mass of the analyte. This can be useful to determine if two analytes will be separated from each other (21).

Capillary electrophoresis can be used for high efficiency separations of peptides and proteins. Numbers of theoretical plates of 10^6 for protein separations have been reported (22). When small capillaries are used in CZE, higher efficiencies are possible because higher voltages can be used. However, detection of the sample zones can be difficult. Therefore, preconcentration methods have been used to facilitate detection in CZE. In the work presented here, an immunoaffinity column was used to selectively preconcentrate a small biomolecule for CZE analysis.

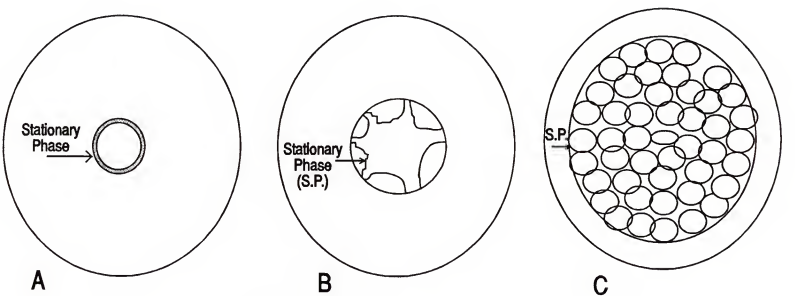

Figure 1-1. Three types of capillary liquid chromatography. (A) is an open tubular, (B) is a partially packed and (C) is a fully packed column.

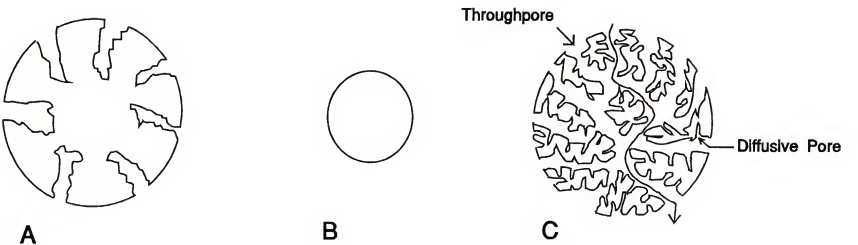

Figure 1-2. Three types of packing material. (A) is a porous particle, (B) is a pellicular particle and (C) is a perfused particle.

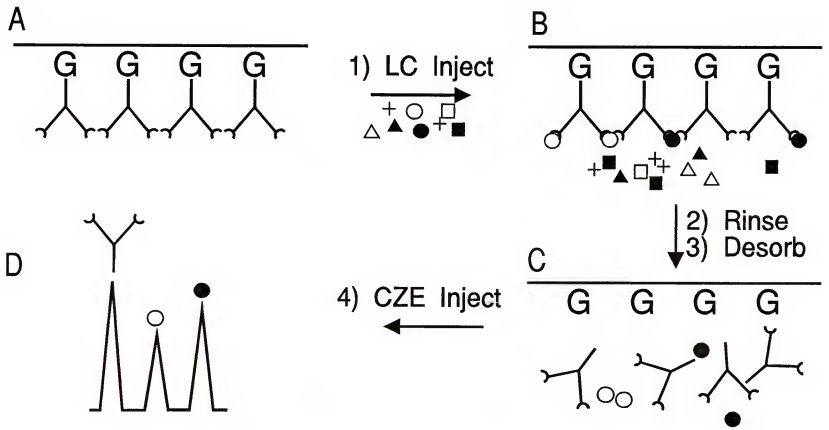

Figure 1-3. Schematic of dual column immunoassay. (A) Protein G column with antibody attached. (B) Antigen binds to the antibody, everything else is rinsed from the column. (C) Antibody and antigens are released from the protein G column by a desorbing buffer. (D) antibody and antigens are separated by CZE.

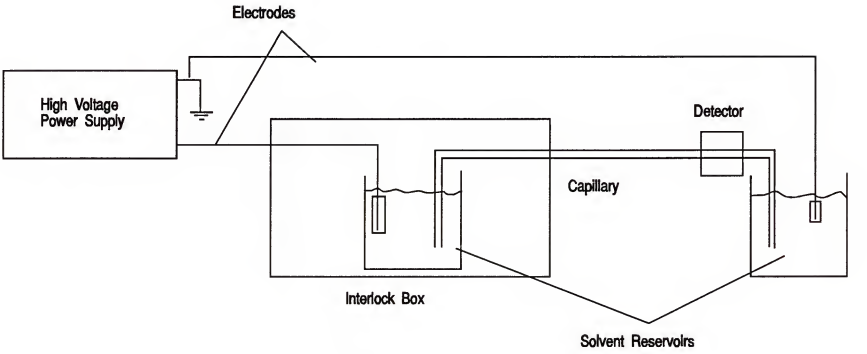

Figure 1-4. Schematic of CZE apparatus.

CHAPTER 2
FAST, PACKED CAPILLARY LIQUID CHROMATOGRAPHY

Introduction

Packed capillary columns have been used in liquid chromatography because of several advantages over larger bore columns. One advantage is that higher numbers of theoretical plates are possible for capillary columns by increasing column length. With this increase in column length comes an increase in separation time. The use of packed capillaries for high speed separations has not been explored to a great extent. This may be because early studies of 100 to 350 μm i.d. microcolumns demonstrated poor performance at high flow rates (23). Recent studies have indicated that capillary columns in the 20 to 150 μm i.d. range have similar kinetic performance as larger columns at high flow rates (1, 2).

A factor in column performance is column diameter to particle diameter ratio (ρ). In previous work, Wilson *et al.* showed with 530 μm i.d. columns and low ρ values, that ρ has a significant impact on column performance independent of column diameter (24). This impact was shown by an improvement in column performance for columns with low ρ values. However, smaller columns' performance under these conditions were not tested. Therefore, it would be interesting to determine if this was also true with small capillaries.

The work presented in this chapter will further explore the possibility that capillary columns will allow separations at high velocities with a higher resolution than with larger

columns. Pellicular and perfused particles are used as packing material in capillary columns to determine 1) if performance will be improved with a decrease in column i.d., and 2) the effect of column diameter to particle diameter ratio (ρ) on performance. In addition, a demonstration of a separation using the best type of column tested is also shown.

Theory

Packed capillary chromatography can allow for higher numbers of theoretical plates than conventional size columns. However, this increase in plates has been achieved at the expense of analysis time by increasing the length of the column. The number of theoretical plates can be given by

$$N = 5.54\left(\frac{t_r}{w_{½}}\right)^2 \qquad \text{Equation 2-1}$$

where t_r is the retention time of the solute and $w_{1/2}$ is the width at half-height of the solute zone (25). Another useful term is the plate height which is given by

$$H = \frac{\sigma^2}{L} = \frac{L}{N} \qquad \text{Equation 2-2}$$

where σ^2 is the zone variance, L is the length of the column, and N is the number of theoretical plates (25). More useful terms are the reduced variables for plate height and velocity because then columns packed with different size particles can be compared since plate height depends on particle diameter and flow velocity. Reduced velocity is given by

$$v = \frac{d_p u}{D_m} \qquad \text{Equation 2-3}$$

where d_p is the particle diameter, u is the linear velocity, and D_m is the diffusion coefficient

of the solute (25). The reduced parameter for plate height is given by

$$h = \frac{H}{d_p} \qquad \text{Equation 2-4}$$

where H is the normal plate height and again d_p is the diameter of the particle (25).

Band broadening at high flow rates limits the speed with which a separation may be performed. One method of evaluating band broadening is based upon the Knox equation shown below (26).

$$h = Av^{0.33} + \frac{B}{v} + Cv \qquad \text{Equation 2-5}$$

The constants A, B and C are determined by the magnitude of band broadening due to eddy diffusion, longitudinal diffusion and resistance to mass transfer, respectively. For conventional size columns (4.6 mm i.d.) packed with porous supports, typical values are A = 1, B = 2, and C = 0.05 (26). Given these parameters, the band broadening due to the C term will be most significant at high flow rates, as shown in Figure 2-1(a). Since the C term includes the resistance to mass transfer in and out of stagnant mobile phase in pores, recent attempts to decrease this term are to reduce the stagnant mobile phase.

There are two methods for reducing the stagnant mobile phase within the pores of the support. First, is to remove the pores completely by using pellicular particles. This approach has a high separation efficiency but column capacity is small compared with porous supports (8, 9, 27). Horvath and co-workers have demonstrated a separation of 5 proteins in 20 s using 2 μm pellicular particles (27). More recently, another approach is to use perfused particles which have a smaller stagnant mobile phase than porous particles (10, 28). A perfused particle is composed of two types of pores. First, is a large

throughpore, which allows the mobile phase to flow through the particle; and the second is a small diffusive pore which increases the surface area of the particle. Using particles of this type, Fulton *et al.* demonstrated a separation of 5 proteins in 15 s (28).

Although the reduction of the stagnant mobile phase is important in decreasing band broadening, there comes a point where other band broadening terms become dominant at high flow rates. When the C term is small, band broadening due to eddy diffusion begins to dominate at high flow rates. For example, a column packed well with pellicular particles is expected to have band broadening terms as follows: A = 1, B = 2, C = 0.003 if stationary phase kinetics are rapid (26). As shown in Figure 2-1(b), at a ν of 150, more than 90 % of the plate height is due to the A term according to the Knox equation.

It has been shown that a decrease in column i.d. can decrease the A term (1, 2). This reduction in plate height has been shown to be a decrease in the eddy diffusion effects and resistance to mass transfer terms. When 5 µm porous particles were packed in 20 µm i.d. capillaries, A terms as small as 0.2 were observed (2). If it is assumed that pellicular and perfused particles packed in capillary columns will exhibit this same decrease in plate height, then the reduction in band broadening due to the A term will result in a significant increase in efficiencies at high velocities. For example, if 5 µm pellicular particles are packed into a 20 µm i.d. capillary, the expected values for the band broadening terms would be A = 0.2, B = 2, and C = 0.003. In a 10 cm long column at a ν of 150, corresponding number of theoretical plates would be 13,300 in a dead time of 5 s. This is in comparison with a conventional column with A = 1, B= 2 and C = 0.003 which would generate 3,800 plates in a time of 5 s. Since resolution increases with the squareroot of

N, a four-fold increase in N means a two-fold increase in resolution, which is a significant increase. Figure 2-2 compares individual terms for capillary columns packed with porous and pellicular particles. As shown in the figure, at a reduced velocity of 150, the porous packed capillary column has 90% of its band broadening due to the C term. The pellicular packed column, in contrast has most of its band broadening at high flow rates from the A term. Therefore, the best possible column should be a capillary column packed with pellicular or perfused particles. This can be demonstrated in Figure 2-3 which compares the theoretical Knox plots for porous and pellicular particles packed in conventional and capillary columns. At a reduced velocity of 150, a five-fold reduction in plate height for pellicular particles packed in capillary columns over porous particles packed in capillary columns is possible. It is expected that perfused particles will exhibit similar properties as pellicular particles since both types of particles have reduced stagnant mobile phase band broadening terms.

Experimental

Chemicals and packing materials. L-ascorbic acid and all buffers and solvents were obtained from Fisher Scientific (Pittsburgh, PA). The perfused particles (10 and 20 μm) were obtained from PerSeptive Biosystems (Cambridge, MA). The 8 and 15 μm glass beads were obtained from Duke Scientific (Palo Alto, CA). Glass beads of 4 μm diameter were obtained from Potters Industries (Hasbrouck Heights, NJ). Methylhydroquinone, 4-methylcatechol, dimethylchloroctadecylsilane and 4 Å molecular sieves were obtained from Aldrich Chemical Company (Milwaukee, WI). 4-Hydroxy-3-methoxyphenylacetic acid was obtained from Sigma Chemical Company (St. Louis, MO).

Column preparation. All columns were prepared according to procedures given elsewhere (2). 30 cm lengths of fused silica capillary (Polymicro Technology, Phoenix, AZ) were used to pack the columns. Before a column could be packed, the capillary had to be prepared with a frit of glass particles in one end. The ends of the capillary were briefly heated with a flame in order to remove the polyimide coating, thereby allowing a viewing window. Frits were made by tapping one end of the capillary into a 1 cm thick pile of glass beads. The diameter of the beads used depended on the i.d. of the capillary. Usually, the diameter of the glass beads were 1/10 to 1/3 the i.d. of the capillary. The beads were then pushed about 0.5 mm into the tube using a 25 μm tungsten wire (Johnson-Mathey, Ward Hill, MA). The tungsten wire was held in place with a micromanipulator (Narishiga MM-333, Southern Microscopes, Orlando, FL). This process was performed while using a stereomicroscope to observe the end of the capillary. After the glass beads were in a satisfactory position and there were no gaps by which the packing could flow through, the beads were heated briefly in a flame until they were sintered in place.

Columns were slurry-packed according to similar procedures shown elsewhere (1, 2). Figure 2-4 shows the apparatus used for packing capillaries. A stainless steel high-pressure bomb (UF Machine Shop) was filled with 0.3 mL of a slurry of particles. As shown in the figure, the bomb allows the inlet of the capillary to be held in the center of the bomb reservoir. In order to pack the columns, a pneumatic amplifier pump (Cat. No. 1666, Alltech, Deerfield, IL) was used. The pressure was increased stepwise from 500 to 2,000 psi over a period of 30 minutes. The pressure was kept at 2,000 psi until the

column had completely packed and then the pressure was turned off. The column was left in the bomb until the pressure had bled through the column. During the packing process, the slurry was stirred using a magnetic stir bar to ensure that the particles were well suspended in the liquid.

Slurry ratios (mL solvent: g packing material) were 100:1. Glass beads were first wet with methanol and then the rest of the slurry was made of 0.5 M KCl. The slurry was sonicated for 2 min before packing with degassed water. Glass beads of 8 and 15 μm diameter were used, although glass beads of 4 μm diameter were also tried. The 4 μm diameter particles were composed of 90% of beads < 6.2 μm, and 10% of beads < 2.0 μm. The beads which were used for the final results had a narrow size distribution: the 8 μm beads were 8.0 ± 0.8 μm with a 16% coefficient of variation (CV) while the 15 μm beads were 15.0 ± 1.1 μm with a 15% CV according to the supplier.

For the perfused particles, both 10 and 20 μm diameter, dried and degassed acetonitrile was used as the slurry solvent. The particles were not sonicated before packing, as this could have destroyed their structure. Also, the highest pressure used for the packing procedure was 2,000 psi as anything higher could result in the destruction of the particles. These particles are spherical and derivatized with a reversed phase stationary phase.

Glass beads were derivatized with dimethylchlorooctadecylsilane as described in Appendix A. These particles were packed with the same procedure as the glass beads previously with one exception: acetonitrile was used as the slurry solvent.

Column testing. Evaluation of the kinetic performance of the columns was performed by measuring the plate height of a nominally unretained solute (ascorbic acid) as a function of flow rate. Ascorbic acid injected was 1 mM. The mobile phase used was 0.1 M phosphate buffer, 5 mM EDTA at pH 5.3. The column packed with reversed phase glass beads was used to demonstrate an actual separation with pellicular particles. In order to determine this a mixture of ascorbic acid, methyl hydroquinone, 4-methylcatechol, and 4-hydroxy-3-methoxyphenylacetic acid of 1 mM each was injected onto the column. The mobile phase used for the reversed phase glass beads was 95 % 0.1 M phosphate buffer, 5 mM EDTA, 100 mM triethylamine at pH 3.0 with 5 % methanol.

Chromatographic system. Evaluation and testing of the columns was performed using a syringe pump (Isco 1000DM, Lincoln, NE) connected to the inlet of the column. The pump was operated in the constant pressure mode. Samples were injected by siphoning into the inlet of the column by raising the sample vial 2 to 10 cm above the outlet of the column. The amount injected was controlled by the amount of time the vial was raised. Extra column band broadening due to the injection was minimized by decreasing the injection time until the plate height did not decrease. The optimum time for injection was typically 5 s. Figure 2-5 shows the schematic for the whole operating system.

Detection. Detection was accomplished by inserting a carbon fiber microelectrode which was 9 μm diameter by 0.5 mm long into the outlet of the column using a micropositioner. This system has been described earlier (2). Figure 2-5 shows the schematic of the detection setup. The column and electrode were inserted into a Lucite

cell which held the mobile phase buffer. The reference electrode used was a sodium saturated calomel electrode (SSCE) and the working electrode was held at +0.70 V vs. the SSCE. A description of the fabrication for the working electrode and reference electrodes is in Appendix B.

Data collection and evaluation. The data were collected using an IBM compatible personal computer (25MHz, 386 from Gateway 2000, Sioux City, SD) interfaced to the detector with a data acquisition board (AT-MIO-16f-5, National Instruments, Austin, TX). The chromatograms were evaluated by statistical moments using software written in our laboratory. The diffusion coefficient for ascorbic acid was estimated to be 5.8×10^{-6} cm^2s^{-1} (29).

In order to evaluate the A and C terms for the columns, the data were fitted to the Knox equation using a non-linear regression analysis program (Systat, Systat, Inc.). It was assumed that B = 2 since there were no points obtained where the B term is significant. The Knox equation is most reliable when the ν range is less than two orders of magnitude; therefore, the data were fit in the ν range of 5 to 150 (26).

Results and Discussion

Characterization of Chromatographic System

Packing evaluation. In order to perform the experiment, columns needed to be packed efficiently and reproducibly. Table 2-1 shows a summary of conditions used to pack glass beads.

Table 2-1: Packing Conditions for Glass Beads.

Slurry solvent	Packing success
Acetonitrile	Did not disperse
2 drops MeOH, Water	Did not pack
2 drops MeOH, 0.1 M KCl	Did not pack well, clogging
2 drops MeOH, 0.1 M Phosphate buffer pH 7	Did not pack well, clogging
2 drops MeOH, 0.5 M KCl	Packed well

The glass beads needed to be wet with an organic solvent at first and then they could be mixed with an aqueous buffer. To aid in the dispersion of the particles sonication of the slurry was used. The best results were with a moderate salt concentration; if this concentration was too high, the particles did not disperse very well. The conditions for the packing of the perfused particles were also explored. Several organic solvents were attempted before the best one was found. A summary is shown in Table 2-2.

Table 2-2: Packing Conditions for Perfused Particles.

Slurry Solvent	Packing Success	Percentage Packed
Methanol	Good	100
Toluene	Plugging of the capillary	0
Benzene	Plugging of the capillary	0
Acetonitrile	Good	100

Although methanol was successful as a slurry solvent, it was found that bubbles formed more readily in the columns packed with methanol than with acetonitrile. In addition to using acetonitrile as the slurry solvent, it was found that the acetonitrile needed to be dried with molecular sieves in order for the packing to be most successful.

Mobile phase composition. The mobile phase composition was an important part of the experimental procedure. Several buffers were tried until an appropriate one was found which gave high numbers of theoretical plates with minimal skew of the peak shape. Table 2-3 summarizes the results from the buffer study.

Table 2-3: Mobile Phase Conditions

Mobile Phase	N	Peak Skew
0.1 M Phosphate buffer, 10% methanol pH 5.3	2000	0.434
0.1 M Phosphate buffer, 10 mM EDTA pH 7	1500	0.431
0.1 M phosphate buffer, 5 mM EDTA pH 5.3	1800	0.222

Although the phosphate buffer at pH 5.3 with both methanol and EDTA exhibited similar numbers of plates, the peak skew was much better with EDTA in the buffer. The peak skew is a measurement of the peak asymmetry from statistical moments. The EDTA in the buffer can complex with any metal ions which come from the metal tubing and connectors. These metal ions are thereby made electrochemically inactive and will not be detected at the electrode surface. Without EDTA in the mobile phase, these metal ions can interfere with the detection of the sample, thereby giving a tailed appearance.

Characterization of Packed Capillaries

Pellicular particles. Figure 2-6 shows Knox plots for capillaries of 50, 75 and 150 µm i.d. packed with 8 µm glass beads. These columns were tested to determine what effect column diameter had on reduced plate height for pellicular particles. Two columns of each size were tested. The 50 and 75 µm i.d. columns exhibit good reproducibility, but the 150 µm i.d. columns did not. It is possible that the smaller i.d. columns were more reproducible because of a wall effect, which states that the column wall imposes an order to the packing arrangement of the particles. This ordering of particles is less dense than the random particle arrangement which is found farther from the walls (30). Since this effect can be observed from 5 to 6 particle diameters from the wall, the smaller capillaries may be dominated by this effect while larger ones would have a mixture of ordered

packing near the wall and random packing in the center of the column. Therefore, this order imposed on the packing may allow more reproducible columns to be prepared.

As well as having better reproducibility than larger columns, the 75 and 50 μm i.d. columns showed an increase in column performance. This is in agreement with work previously published using porous particles packed in capillary columns (1, 2). The best results were obtained with the 50 μm i.d. capillary which had a minimum plate height of 0.86. At a high reduced velocity of 289, h was 4; this corresponds to 6,700 plates in a time of 10.1 s or 666 plates s^{-1} for an unretained solute. This is the highest value of plates per second reported for a packed capillary column. If even smaller particles of 3 or 5 μm diameter were used instead of 8 μm particles, an improvement of 2,000 or more plates s^{-1} could be realized. Unfortunately, none were available.

Figure 2-7 shows Knox plots for 15 μm particles packed in 50, 75, 100 μm i.d. capillaries. It is important to determine whether larger pellicular particles would yield similar results as the 8 μm glass beads for the effect of column diameter on plate height. The results are similar to those found for columns packed with 8 μm particles. Only one example of each size capillary is shown. Capillaries of 150 μm i.d. were not attempted, since the results with the 8 μm glass beads were not reproducible. The best results were attained with a 50 μm i.d. column which had a minimum reduced plate height of 0.54. At ν of 1065, the reduced plate height was 3.8. This corresponds to 5200 plates for an unretained solute eluting in 7.04 s which gives 745 plates s^{-1}. Although the number of plates is lower than with the 8 μm particles at a comparable reduced plate height, the plates per second value is higher.

As explained in the Experimental section, plate height data were fit to the Knox equation in order to determine the A and C terms. These terms were calculated for 8 μm particles in 50 and 75 μm i.d. capillaries, and for 15 μm particles packed in 75 μm i.d. columns. The results are summarized in Table 2-4.

Table 2-4: Calculated Column Parameters.

Column i.d. (μm)	d_p (μm)	ρ	A[a]	C[a]	Φ[b]
75	8	9.4	0.59	0.022	208
75	8	9.4	0.59	0.013	232
50	8	6.7	0.37	0.010	258
50	8	6.7	0.37	0.007	368
75	15	5.0	0.31	0.004	242
75	15	5.0	0.31	0.005	295

[a]Coefficients calculated from the Knox equation as described in the experimental Section.
[b]Calculated as given in reference 31.

It is shown that both the A and C term decrease with the column diameter as was expected according to results previously found with 5 μm porous particles (1, 2). The A terms for these capillaries are better than for conventional size well-packed columns, although they are not as low as for 5 μm porous particles in 20 μm i.d. capillaries (2). The C term, however, was not as small as the theory would predict; although it did approach the value of 0.003 with smaller column diameters. The data show that the A and C term can be decreased simultaneously by using pellicular particles packed in microcolumns to obtain high numbers of plate s^{-1}.

Effect of column diameter to particle diameter ratio. The different i.d. columns packed with 8 μm particles also varied in their column diameter to particle diameter ratio (ρ). The relative importance of column i.d. and ρ in improving performance of the columns was evaluated by using a 75 μm i.d. column packed with 15 μm particles. Figure

2-8 compares 75 μm i.d. columns packed with 8 and 15 μm glass beads. By using the same i.d. capillary packed with different size particles, the importance of ρ to the performance of the column was determined. The column packed with 15 μm particles has a smaller ρ than those packed with 8 μm particles. As shown in Figure 2-8, the column with the smaller ρ has better performance than the columns with higher ρ values. This trend of better performance is also reflected in the A and C term values, as Table 2-5 shows. A 50 μm i.d. column packed with 8 μm particles was also examined for ρ effects by comparing with 75 μm i.d. columns packed with 8 μm or 15 μm particles. The ρ of this column was similar to the 75 μm i.d. column packed with 15 μm particles. As expected, this column has a performance comparable to the other column but better than the 50 μm i.d. column. Therefore, it appears that ρ has a significant role in column performance, independent of column inner diameter. Wilson, *et al.* reached a similar conclusion with work performed on 530 μm i.d. columns and low ρ values (24).

The smallest particles which were studied were 8 μm. Smaller particles of 4 μm size were explored, but the columns packed with these particles clogged easily. This may be because of the large range of sizes contained within the bulk packing material. These particles could have been fractured under the high pressures used for packing, thereby producing fines. A fine is when the particle is splintered into very small shards. However, it may be of interest to determine whether this trend of improvement with smaller ρ holds for smaller particles packed in smaller columns. Columns with ρ smaller than those shown here were attempted; however, during the packing process, these columns tended to have particles caught in the column which could not be moved despite using sonication and high

bursts of pressures. Improvements in column packing techniques could allow columns with smaller ρ to be prepared.

It is unclear how small ρ values could cause improved column performance. One possible explanation is that with the smaller column i.d., only the smaller particles in the slurry are allowed into the column. However, this does not seem to be the case since the size distribution for the particles used is very narrow. Also, it would be expected that if smaller particles were packed in the column, that the flow resistance parameter (Φ) would increase with decreasing ρ (31). The flow resistance parameter, which is a unitless parameter, measures the resistance to flow of the mobile phase for a column. The flow resistance parameter is described by

$$\phi = \frac{\Delta P d_p^2}{\eta u L} \qquad \text{Equation 2-6}$$

where ΔP is the column pressure drop and η is the solvent viscosity (31). Therefore, if the particle diameter was not the expected size, then Φ would increase . However, this trend was not observed as shown in Table 2-5.

The improvement in performance is likely to be inherent to columns with low ρ values. For the decrease in A term with ρ, it can be rationalized by considering what the A term results from. The A term is due to the multiple flow paths which occur transchannel, transparticle, short-range interchannel, long-range interchannel, and transcolumn (32). By reducing the number of particles across the diameter of the column, the possibility for long-range interchannel, short-range interchannel and transcolumn flow path variations are reduced. The apparent decrease in the C term could be a result of the

coupled nature of the A and C term which makes it difficult to differentiate mobile phase effects by simple curve fitting.

Perfused particles. The use of columns packed with perfused particles was also evaluated. Perfused particles should exhibit similar characteristics to pellicular particles, therefore similar studies were performed. Capillaries with i.d. of 50, 75, 150 and 250 μm were packed with 10 and 20 μm perfused particles. Figure 2-9 is a Knox plot of one of each column i.d. tested. The data from the 75, 150, and 250 μm i.d. columns all lie on the same line. The 50 μm i.d. column is only a small amount lower than the rest of the columns. These columns showed much less dependence on column i.d. than the pellicular particles. This discrepancy is surprising and difficult to explain.

Although column i.d. did not have an effect on the performance of capillaries packed with perfused particles, the capillary columns did exhibit improved performance over that of a commercially available 2.1 mm i.d. by 30 mm length column. One of these size columns was tested by Afeyan *et al.* and the data are plotted in Figure 2-9 (10). The data from the smaller diameter capillaries gave better performance than the 2.1 mm column. The large column was tested with adenosine monophosphate and the mobile phase was 0.1 M phosphate buffer pH 2.6 and the stationary phase was ion-exchange (10). Although the conditions were somewhat different, the fact that an unretained solute was used for testing and that reduced parameters were used allows for a reasonable comparison. As shown in Figure 2-9, the behavior of the large bore columns are different than the capillary columns. The effect of perfusion can be readily seen with the large bore columns as h becomes independent of v. The capillary columns start at much lower plate height values, but the

plate height never becomes independent of v. It is not clear why the capillary columns perform differently than the large bore columns. It could be that with smaller A terms, the small dependence of h on v is more easily observed.

Figure 2-10 shows a Knox plot for 10 μm particles packed in 40, 50, 75, 150 i.d. capillaries. Although 20 μm particles did not show an improvement with decreasing column i.d., 10 μm particles were tested to determine if particle diameter had an effect on performance. As shown, all of the different capillary sizes fall on the same line. Even though the results were not the expected ones, the columns' performance was good. The best results for these columns were obtained with a 50 μm i.d. capillary where the minimum h was 0.88. It was possible to achieve 140 plates s^{-1} with a 50 μm column packed with 10 μm particles.

Figure 2-11 shows a comparison of 10 and 20 μm particles packed in 75 μm i.d. capillaries. Although there was no dependence on column i.d. for these perfused particles, there still might have been a dependence on ρ. However as shown in Figure 2-11, there seems to be no dependence on ρ with the perfused particles as there was with the pellicular particles.

Comparison of column types. Figure 2-12 shows a comparison of 50 μm i.d. columns packed with 5 μm porous particles, 8 μm pellicular particles and 10 μm perfused particles. (The data for the porous particles, obtained from reference (2), should be viewed with some caution as data were only collected up to v of 30 using nitrite ion as the test solute. The rest of the data points were extrapolated based on the Knox equation and best fit values for the A, B, and C terms.) As shown, pellicular and perfused particles give

much better performance than the porous particles at high flow rates. For example, at a v of 100 reduced plate heights are 17, 4.6, 2.4 for porous, perfused and pellicular respectively. Columns packed with pellicular and perfused particles give similar performance over the range tested. Therefore, the data clearly show the advantage of using perfused and pellicular particles over porous particles. Smaller pellicular particles could be used in order to achieve higher numbers of theoretical plates.

Demonstration of a separation. A qualitative demonstration of a separation was performed using a 29 cm long, 50 μm i.d. column packed with 8 μm pellicular particles derivatized with octyldecylsilane. These column dimensions were used because they were observed to give the highest plates s^{-1}. Figure 2-13 shows the chromatogram using ascorbic acid, methylhydroquinone, 4-methylcatechol, 4-hydroxy-3-methoxyphenylacetic acid. As shown in Figure 2-13, these small compounds were separated in less than 75 s; this shows that rapid separation of these small compounds are possible using relatively large particles packed in capillaries. An even larger advantage should be realized for the separation of proteins.

Concluding Remarks

Based on the types of packed capillaries tested in this chapter, it was found that the reduced plate height decreased with a decrease in column i.d. for pellicular particles. This conclusion supports similar work performed with columns packed with porous particles (1,2). An unretained solute was eluted from a 50 μm i.d. capillary packed with 8 μm pellicular particles in 10.1 s with 6,700 theoretical plates. It was determined that when ρ was decreased, better column performance was observed within the range of column i.d.

tested. Finally, although it was expected that perfused particles would exhibit the same characteristics as pellicular particles, there was not a dependence on column i.d. or ρ. However, the capillary columns packed with perfused particles tested in this chapter did show an improvement in performance over a 2.1 mm i.d. column (10).

The high speed, high resolution separations suggested by these results as well as the small sample requirements indicate several possible applications for these capillary columns. For instance, they could be used for sensor-like applications for time resolved monitoring of multiple compounds.

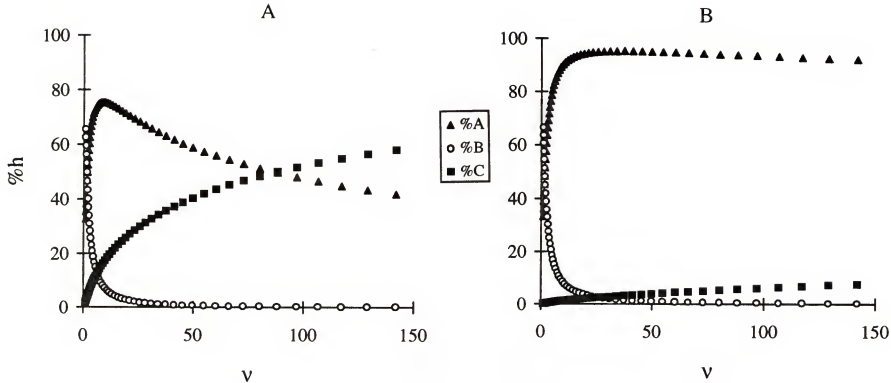

Figure 2-1. Reduced plate height as a function of reduced velocity for (A) a conventional size column packed with porous particles (A = 1, B = 2, C = 0.05), and (B) a conventional size column packed with pellicular particles (A = 1, B = 2, C = 0.003).

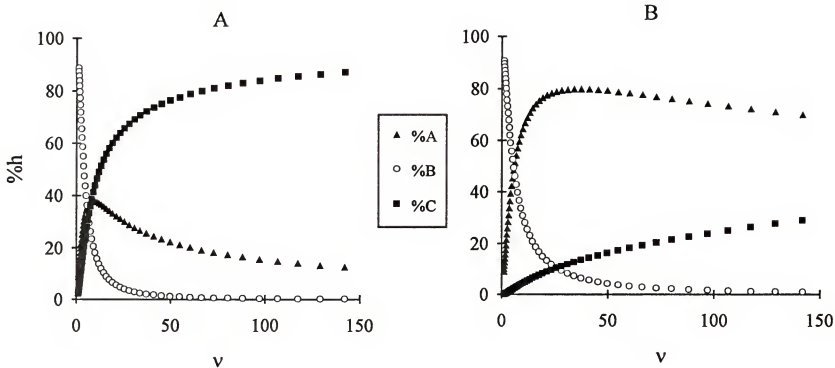

Figure 2-2. Percentage of reduced plate height as a function of reduced velocity for capillary columns packed with (A) porous particles (A = 0.2, B = 2, C = 0.05) and (B) pellicular particles (A = 0.2, B = 2, C = 0.003).

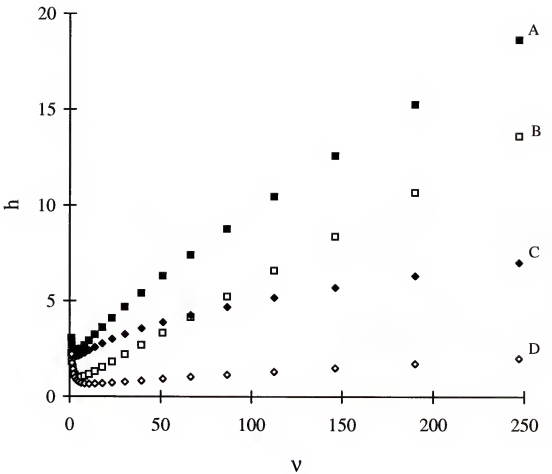

Figure 2-3. Reduced plate height as a function of reduced velocity for a theoretical comparison of the efficiencies of porous particles packed in (A) conventional size columns and (B) capillary columns and pellicular particles packed in (C) conventional size columns and (D) capillary columns.

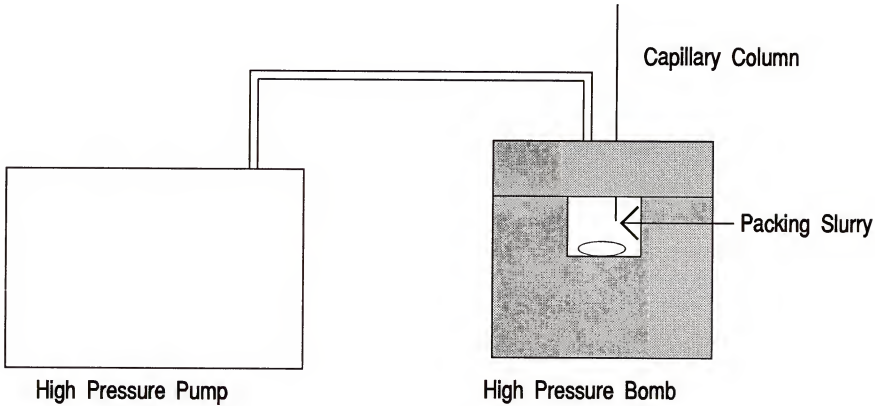

Figure 2-4. Schematic of the apparatus used to slurry pack capillary columns.

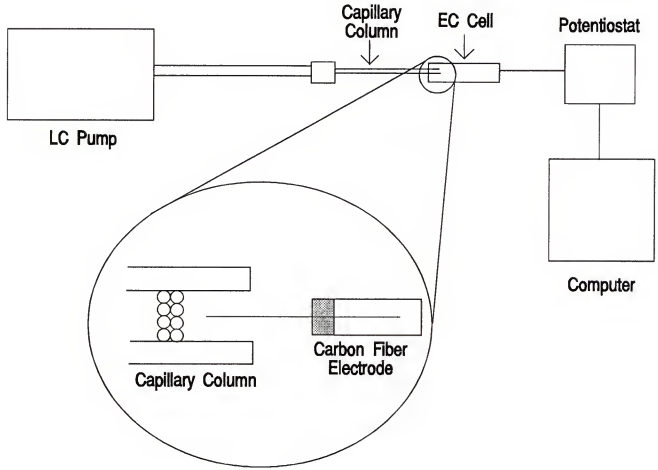

Figure 2-5. Schematic of the apparatus used to test capillary columns. The blown up section depicts the electrode inserted in the end of the capillary.

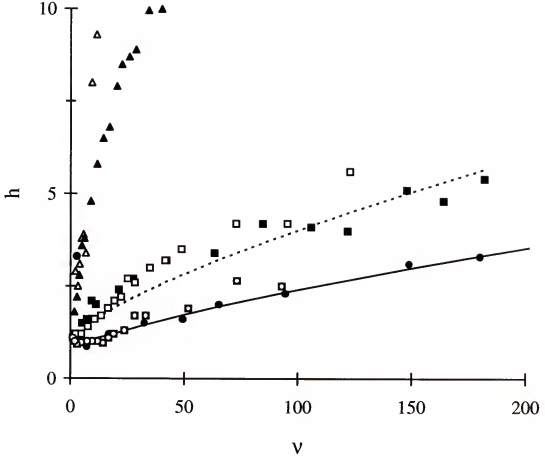

Figure 2-6. Knox plots for 8 µm glass particles packed in various size capillaries. Reduced plate height is plotted as a function of reduced velocity. The triangles are 150 µm i.d.; the squares are 75 µm i.d.; the circles are 50 µm i.d. Two columns were tested for each size capillary. The lines through (■) and (●) represent the best fit line from the Knox equation.

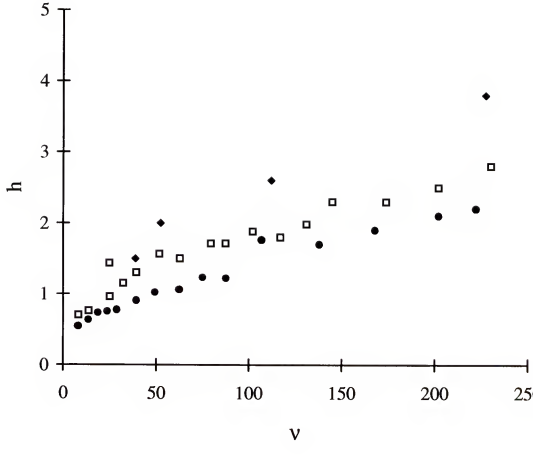

Figure 2-7. Knox plots for 15 μm glass particles packed in various size capillaries. Reduced plate height is plotted as a function of reduced velocity. The capillaries shown are (◆) 100 μm i.d.; (□) 75 μm i.d.; (●) 50 μm i.d. One plot from each size column is shown.

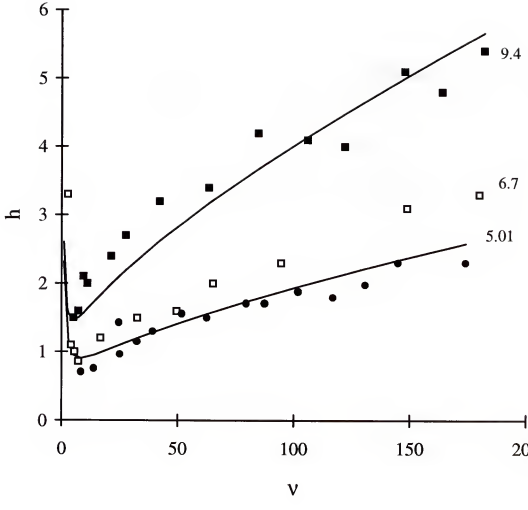

Figure 2-8. Comparison of columns with different ρ values. Plate height, h, as a function of reduced velocity, ν, is shown for (■)75 μm i.d., 8 μm d_p; (●)75 μm i.d., 15 μm d_p; (□) 50 μm i.d., 8 μm d_p. The number beside each data set is the ρ value for that column. The lines through the 75 μm i.d. columns are the best fit lines to the Knox equation.

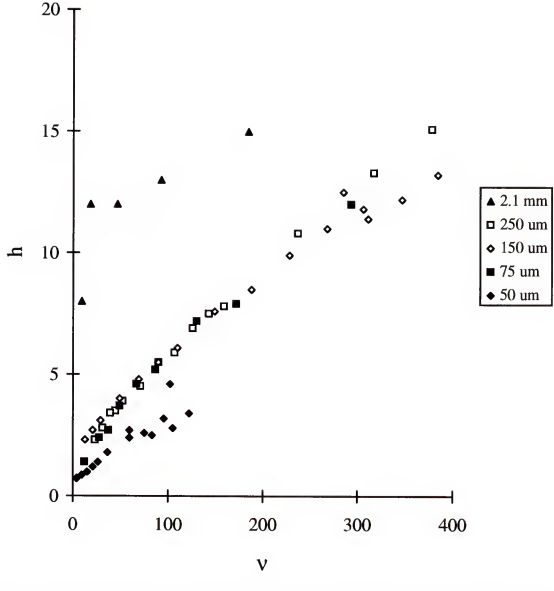

Figure 2-9. Plate height, h, as a function of ν for 20 μm perfused particles packed in 2.1 mm i.d. to 50 μm i.d. columns.

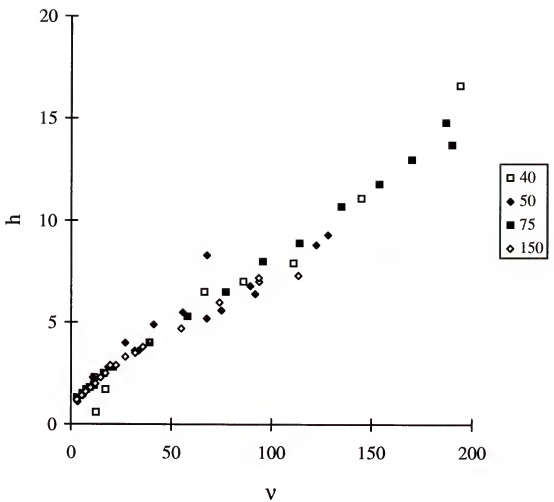

Figure 2-10. Plate height, h, as a function of v for 10 μm perfused particles packed in 40, 50, 75 and 150 μm i.d. capillaries. Data from a representative capillary are shown for each size.

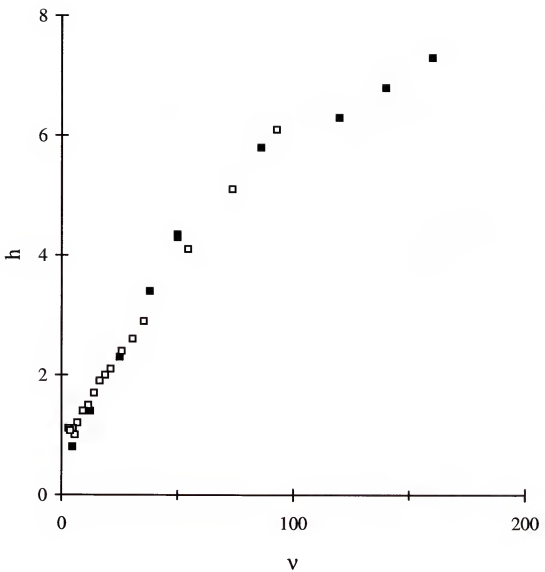

Figure 2-11. A comparison of 10 (□) and 20 μm (■) perfused particles packed in 75 μm i.d. columns. Plate height, h, as a function of ν is shown.

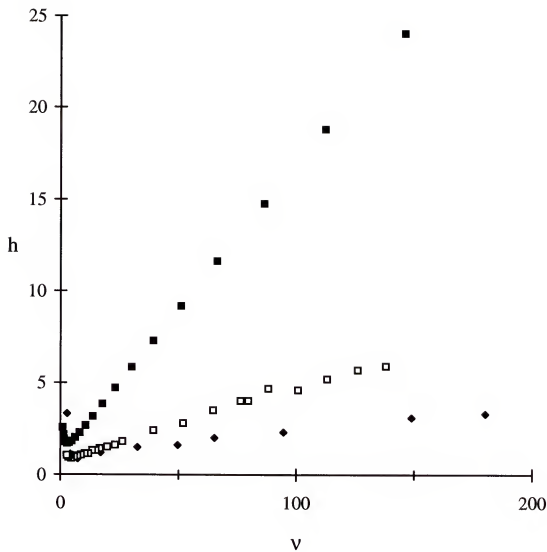

Figure 2-12. Plate height, h, as a function of v for 50 μm i.d. columns packed with (■) 5 μm porous, (□) 10 μm perfused, and (◆) 8 μm pellicular particles. The data for the porous column were extrapolated from actual A, B, and C terms calculated using nitrite ion as an unretained test solute (2). The actual data had a v max of 30. The perfused and pellicular particles data was obtained from this work.

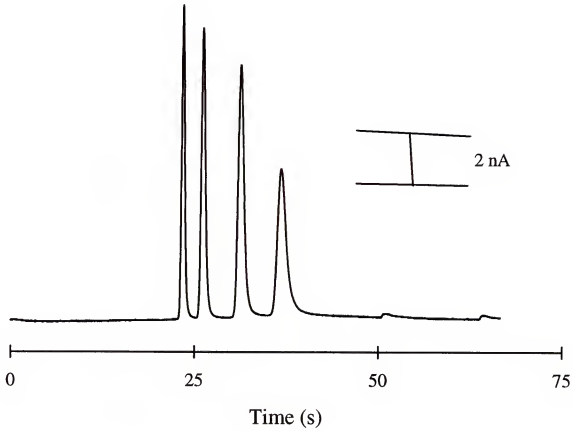

Figure 2-13. Chromatogram illustrating a separation with reversed phase derivatized 8 μm glass beads packed in a 50 μm i.d. capillary. The mobile phase was 95% 0.1 M KH_2PO_4, 5 mM NaEDTA, 100 μM triethylamine at pH 3.0 and 5% methanol. The compounds were eluted in the following order: ascorbic acid, methylhydroquinone, 4-methylcatechol, 4-hydroxy-3-methoxyphenylacetic acid.

CHAPTER 3
A SELECTIVE PRECONCENTRATION METHOD FOR CZE

Introduction

The difficulty of detecting separated zones in small capillaries used with capillary zone electrophoresis (CZE) has led to considerable efforts in the development of preconcentration methods that are compatible with CZE (33-49). Three distinct methods for preconcentration onto CZE columns have been utilized. One is sample stacking where samples dissolved in a low ionic strength media are preconcentrated by virtue of the higher electric field they experience during electrokinetic injection (40-42). Other methods use isotachophoresis in which a plug of sample in a capillary is sandwiched between electrolyte of high mobility and one of low mobility (33-39). Finally, chromatographic sorbents, typically reversed-phase type, have been used as preconcentrators (43-49).

A common characteristic of all of these methods is that they preconcentrate with low selectivity. In some cases this is desirable; however, in other cases the preconcentration of unwanted substances present at high concentrations may tend to obscure peaks due to compounds of interest present at low concentrations. In these circumstances, preconcentration of only the analytes of interest would be beneficial. Some efforts at enhancing selectivity of the preconcentration step have been made. For instance, appropriate choice of the leading and terminating electrolytes during isotachophoresis preconcentration has allowed the rejection or selective preconcentration of certain ions

from samples prior to a CZE separation (39). Of the methods available however, chromatographic preconcentration would seem to have the greatest opportunity to selectively preconcentrate analytes because of the wide range of sorbents that are available. For example, a metal chelate chromatographic sorbent has been used to selectively preconcentrate metal binding proteins for CZE analysis (46). For the work presented in this chapter, an immunoaffinity chromatography column has been used to selectively preconcentrate insulin for CZE analysis (18). In another case, highly selective preconcentration of amphetamine from urine for CZE analysis was achieved using immunoaffinity columns (43). One of the goals of the present work was to explore the analytical aspects of immunoaffinity preconcentration for CZE.

Immunoaffinity chromatography is a specific type of affinity chromatography. Affinity chromatography uses immobilized molecules to separate the analyte of interest from the whole sample. The immobilized molecule needs to bind reversibly and selectively to the analyte. Some typical affinity ligands are antibodies, enzyme inhibitors and lectins. Affinity ligands can be divided into two categories of binding: specific and group-specific. An antibody would be considered specific, since it should bind to only one solute. On the other hand, ligands which will bind to a class of solutes are in the group-specific category.

An important consideration for affinity chromatography is the support. Supports which are commonly used in affinity chromatography are agarose, cellulose, and dextran gels. Agarose gels are the most commonly used. However, other supports such as silica-based or size exclusion can be modified and used for affinity chromatography. Before the affinity ligand can be bound, the support must be activated to facilitate binding of the

ligand. After activation the affinity ligand, in the present case antibody, is immobilized by covalent bond formation between the activated support and the ligand. Once the affinity ligand is bound to the support, the analyte is rinsed through the column. Elution of the solute can take two forms: biospecific or nonspecific. In a biospecific elution, a mobile phase modifier is used which is similar either to the analyte or the ligand. This modifier then competes with either the analyte or the ligand for binding. This will reduce the capacity factor (k') of the analyte, allowing it to be eluted. In the nonspecific mode, elution is brought about by means of pH, organic solvents, or ionic strength. The affinity support should not be damaged from the elution agent.

An affinity support can be used to bind antibodies. Antibodies are a family of glycoproteins that share structural and functional relationships (50). An antibody is composed of one or more copies of a Y-shaped structural unit. An example of one such unit is given in Figure 3-1. Each unit is composed of two identical light chain regions and two identical heavy chain regions. The heavy-chain polypeptides have a molecular weight of 55,000 daltons while the light-chain polypeptides have a molecular weight of 25,000 daltons each. One light-chain and the amino-terminal of the heavy-chain combine to form an antigen binding region. The polypeptide chains are held together by disulfide bridges and noncovalent bonds. There are three distinct regions of each unit. The arm-like fragments are called the Fab fragments and each arm has an antigen binding region. These Fab fragments can be dissociated from each other and the third domain by cleavage with papain. The base of the unit is the Fc fragment which is involved in the immune response of the antibody. The most abundant antibodies in serum are IgG antibodies which contain

one Y unit. An affinity support modified with protein G, a bacterial protein, binds IgG at the Fc region which orients antibody with the antigen binding region away from the surface (51). An immunoaffinity column which has an IgG antibody attached will be used to preconcentrate insulin for CZE analysis.

Some chromatographic preconcentrators have been prepared by packing a small section of the CZE capillary with a chromatographic sorbent (47, 49). This is beneficial in that it eliminates the need to couple two microcolumns; however, it does constrain the system. For instance, all compounds injected onto the preconcentrator must come through the CZE capillary. This is undesirable if some sample components, such as adsorbing proteins, are deleterious to the CZE capillary. In addition, the preconcentrator must be small enough that it does not cause excessive band broadening in the CZE separation. This tends to limit the amount of preconcentration that is possible with the chromatographic sorbent. Band broadening can be caused by slow desorption kinetics in this system thus preventing the use of some sorbents as preconcentrators. Finally, any solution passed through the capillary must be compatible with both the preconcentrator and the CZE capillary. To avoid these problems, some groups have reported the use of on-line preconcentrators which are separate from the electrophoresis capillary. The chromatographic bed has been incorporated into an injection valve (44) or a separate capillary (43,45,46,48) from which injections can be made onto the CZE capillary. For the work presented in this chapter, the chromatography bed will be in a separate capillary from the CZE capillary.

Three types of chromatography columns are explored for use as preconcentrators for CZE. The first type used is a protein G modified support which has antibody noncovalently attached. With this type of column, both antibody and antigen are eluted from the column. Therefore, harsh conditions are used to be certain that antibody and antigen do not recombine on the CZE column. Once the protein G noncovalent columns were tested and used, a covalent column was tested. It was desirable to remove the antibody from the CZE separation in order to use better CZE buffers. The total analysis time included antibody and antigen loading steps. The analysis time could be reduced by removing the need to load antibody after every desorption step. These protein G, noncovalent columns worked well for preconcentrating insulin from dilute samples.

The second type of column used is an epoxide activated support with antibody covalently attached. This type of column did not give as high sample capacities as the protein G non-covalent. Therefore, the protein G columns are used; but, the antibody was attached covalently with a cross-linker. Both types of protein G columns are used on-line and off-line as preconcentrators for CZE.

In this chapter, a system in which a packed capillary immunoaffinity column is coupled to CZE with UV-VIS absorbance detection is described. Both off-line and on-line coupling are utilized with protein G columns. On-line coupling is performed using an interface first described by Lemmo and Jorgenson (3) for two-dimensional separation systems. The performance of the chromatographic preconcentrator and the combined system are explored. Bovine insulin is used as the test analyte. The system allows highly selective preconcentration from complex samples. Preconcentration factors of at least

1,000 are attained for insulin and the amount of preconcentration is easily predicted if the system is operated in the off-line mode.

Experimental

Chemicals. Polybrene and tricine were from Aldrich Chemical Co. (Milwaukee, WI). Dimethylpimelimidate was from Pierce Chemical Co. (Rockford, IL). All other chemicals and serum samples used for buffer preparation and standards were from Sigma Chemical Co. (St. Louis, MO). Insulin refers to bovine insulin for all experiments reported here.

Chromatographic column preparation. Chromatographic packing material was POROS 20G and POROS 20 EP (PerSeptive Biosystems, Cambridge, MA). POROS 20G is a perfusive support with a 20 μm particle diameter modified with recombinant protein G. POROS 20 EP is also a perfusive support with 20 μm particle diameter, but modified with epoxide rings. Columns were prepared and packed as described in Chapter 2. The columns were packed at a lower pressure than the columns in Chapter 2. The bomb pressure was increased to 1000 psi over a period of 5 min. Columns packed were 5-10 cm in length and slurry ratios (mL solvent: g packing material) of 80:1 were used with distilled water as the slurry solvent for protein G columns. The slurry solvent for epoxide activated support was 0.2 M Tris buffer at pH 9.4.

Antibody was loaded onto packed protein G columns by injecting a solution of 2.3 μM antibody diluted in loading buffer. The loading buffer consisted of 0.05 M sodium phosphate, 0.05 M potassium sulfate pH 6.8. Flow rates for loading were 10 μL/min unless stated otherwise. Desorption of antibody and insulin were accomplished by

injection of desorbing buffer which consisted of 0.1 M glycine, 0.05 M sodium phosphate, 20% acetic acid pH 3.

Antibody was covalently attached to epoxide activated support before packing of the column. Antibody was diluted to a concentration of 6.3 μM in 0.1 M sodium borate buffer pH 9.45 and then exchanged with 900 μL of 0.1 M sodium borate with a Centricon centrifuge to remove any excess amines in the solution. A 2 M solution of sodium sulfate pH 9 was added to the antibody solution to achieve salting out of the antibody onto the support. Epoxide activated particles were added and allowed to react overnight with the antibody with gentle stirring. Figure 3-2 describes the general reaction mechanism for the binding procedure of antibody to support. Any residual epoxide functionality was quenched by reacting the particles with 0.2 M Tris buffer pH 9.45. The Tris buffer contains amines which will react with the oxirane ring and cover the binding spots. This procedure was modified from instructions provided by the supplier of the particles. The instructions from the supplier gave general conditions, but not concentrations or pH of buffers. In general, recommended buffers are carbonate, borate or phosphates at pH higher than 9. Therefore, a 0.1 M sodium borate buffer was used. Insulin was loaded in the same buffer as for protein G columns; however, the desorbing buffer was 0.05 M sodium phosphate, 0.05 M potassium sulfate pH 3.

Antibody was also covalently attached to packed protein G columns using a crosslinking polymer (52). The crosslinker used was 25.5 mM dimethylpimelimidate in 0.2 M triethanolamine pH 8.2. The crosslinking solution was flowed through the column at 200 psi for 30 min. Then 0.1 M ethanolamine pH 8.2 was rinsed through the column at

500 psi for 10 min. Finally, 0.05 M sodium phosphate, 0.05 M potassium sulfate pH 3 was rinsed through the column to remove any noncovalently bound antibody. Insulin was loaded in the same buffer as previous onto the protein G column and the same desorbing buffer was used as in the epoxide activated columns.

The antibody used in this work was a mouse monoclonal IgG_{2a}. The antibody was produced from a hybridoma line originally developed by Schroer *et al.* (53) and was obtained from the American Type Culture Collection (ATCC HB 124, Rockville, MD). Schroer *et al.* have reported that the antibody has an affinity constant of 5×10^7 L/mol for insulin (53). The antibody cross-reacts with insulin from human, beef, pork, rabbit, rat, and chicken. Antibody was obtained at 50 mg/mL in phosphate buffered saline from protein G affinity chromatography purification of mouse ascites fluid from the University of Florida Hybridoma Laboratory.

The theoretical saturation point of insulin binding for protein G columns (covalent and noncovalent) was calculated using the following equations:

Volume (vol) of packing (mL) = $\pi r^2 L = \pi(75 \times 10^{-4}\ \text{cm})^2(10.5\ \text{cm}) = .00186$ mL

Theoretical IgG binding capacity (cap) = 10 mg IgG/1 mL packing

Moles (mol) of antibody (Ab) bound to column = (vol × cap)/MW Ab

$= (0.00186\ \text{mL})(10 \times 10^{-3}\ \text{g/mL})/160{,}000$

= 116 picomoles

Insulin capacity (concentration) = (mol of Ab) × 2/vol injected

$= (116 \times 10^{-12}\ \text{mol})(2)/20 \times 10^{-6}\ \text{L} = 11.6\ \mu\text{M}$

The example given above used a 10.5 cm long column injected with 20 μL of insulin solution. The theoretical IgG binding capacity of the protein G support was obtained from the supplier of the support.

Chromatography column characterization. Chromatography columns were characterized using a system consisting of a syringe pump (ISCO 1000DM, Lincoln, NE) operated in the constant flow mode, connected in series to a 6-port injection valve (C6W, Valco Instruments Co. Inc., Houston, TX). A conventional 1/16" ferrule fitting was used to connect the column to the injection valve. To make a leak-free connection, it was necessary to insert a 1 cm section of the column at the inlet into a teflon tubing (1/16" o.d. by 0.010" i.d.) sleeve. Detection was accomplished using a UV absorbance detector (Spectra 100 from Spectra-Physics, Fremont, CA) at 280 nm for the protein G columns. For the epoxide activated and covalent protein G columns, 210 nm was used. Data were collected at 10 Hz using an IBM-compatible 25 MHz 386 personal computer (Gateway 2000, Sioux City, SD) interfaced to the detector with a data acquisition board (AT-MIO-16f-5, National Instruments, Austin, TX). Chromatograms were evaluated by statistical moments using locally written software.

Affinity LC coupled with CZE. Experiments performed with "off-line" coupling consisted of collecting fractions from the immunoaffinity column and subsequent injection from these fractions onto the CZE column. Fractions were collected manually in glass microvials. Timing of fraction collection was determined by performing test runs with the UV detector on the chromatography column. During actual fraction collection however, the detector was removed and collection performed based on the expected retention time.

Collected samples were injected onto the CZE column hydrodynamically by raising the sample vial 5 cm for 60 s. Unless stated otherwise, the CZE capillary was a 80 cm length of 50 μm i.d., 350 μm o.d. fused silica (Polymicro Technologies). The inner surface of the capillary was coated with polybrene using the following protocol: 1) rinse capillary with 0.1 M NaOH for 15 min, 2) rinse capillary with H_2O for 5 min, 3) rinse capillary with 10% w/w polybrene in H_2O, 4) allow polybrene solution to stand overnight in column, and 5) rinse column with H_2O and the migration buffer for 5 min each (54). Unless stated otherwise, migration buffer was the same as the desorbing solution. The injector to detector distance was typically 20 cm and the electric field strength was 190 V/cm. Voltage was applied using a Spellman CZE 1000R (Plainview, NY). On-column UV detection was performed at 210 nm for CZE separations. All other aspects of detection, data collection, and analysis were performed using the same equipment and software as for the chromatographic characterizations.

For on-line analysis, the immunoaffinity column was coupled to the CZE column using a flow-gated interface (3). An overview of the on-line system is shown in Figure 3-3. The heart of the system is the interface which is described in detail elsewhere (3). Briefly, the interface juxtaposed the LC column outlet and the CZE column inlet inside a flow channel with a separation distance of approximately 75 μm. Migration buffer for the CZE was driven by gas pressure through the flow channel perpendicular to the capillaries to waste. Thus flow of migration buffer is the gating-flow. The gating-flow supported the electrophoresis and washed LC column effluent away from the CZE inlet thus preventing it from entering the CZE capillary. To inject a fraction from the LC column, the gating-

flow was stopped by a valve thus allowing column effluent to build up in the channel between the LC and CZE columns. An injection voltage was applied to the CZE capillary (5 kV for 60 s). After electrokinetic injection, the voltage was turned off, the gating-flow resumed, and the separation voltage applied. This system has been demonstrated to allow injection of samples flowing from capillaries with no dilution and no extra-column band broadening (3, 55). The system also prevents effluent from the chromatography column from entering the CZE capillary except when desired. Thus, all of the necessary affinity column manipulations such as antibody and sample loading could be performed with no effect on the CZE capillary. The time to start the injection onto the CZE system was determined experimentally by varying the time until the largest analyte peak was observed. For all on-line experiments, the CZE capillary was 80 cm total length, with a 20 cm effective length, 25 μm i.d., and E = 313 V/cm. The migration buffer was the same as the off-line case.

Results and Discussion

Characterization of Protein G - Noncovalent Columns

For the work described here, the chromatographic support consisted of a perfusion-type particle modified with protein G. Protein G binds immunoglobulins through noncovalent interactions. For this reason, protein G, and the related protein A, is usually used as an affinity stationary phase for the purification of immunoglobulins. However, if loaded with antibody these proteins can also be used as an immunoaffinity stationary phase for an antigen (15, 56). This chromatographic support has several characteristics which make it suitable for preconcentration applications. First, it has a high capacity which

allows large preconcentrations to be achieved. Second, the particles are large (20 μm diameter) which makes them compatible with high flow rates which is important for rapid loading of large samples. Third, perfusion of the particles reduces stagnant mobile phase effects and thereby enhances kinetics of binding to the surface which also allows for rapid loading of antibody and sample onto the column (10, 57). Fourth, protein G binds antibody at the Fc region which orients antibody with the antigen binding regions away from the surface and towards solution (58). Proper orientation of the antibody enhances specific activity of the antibody (57, 59). Fifth, the protein G support is versatile in that it binds a wide variety of antibodies and can be used to simply produce columns with different selectivities. Thus, the same column can be used to preconcentrate different analytes by changing the antibody between analyses (15).

Subtraction assay. To determine whether the protein G column was binding antibody and that the antibody was binding insulin, a subtraction assay was performed (60). It was necessary to use the subtraction assay since injection of a desorbing solution causes loaded antibody and captured insulin to elute simultaneously. Thus, it was difficult to determine the amount of insulin that was captured by examining the elution of the desorbed zone since this zone was dominated by antibody. To illustrate the subtraction assay, Figure 3-4 shows chromatograms from 1 μM insulin samples. The sample injection is monitored until all of the sample is rinsed through the column. The greatest peak height and area is when no antibody is bound to the column. As expected, the peak height and area decrease when antibody is bound to the column. For calculating the peak height difference, the blank peak height is first subtracted from all the data and then the

difference between the two insulin peaks are calculated. It is not clear why there is such a large difference between the blank and the insulin after antibody was loaded onto the column. Theoretically, the peak heights should have been the same. In later experiments, it is shown that the blank and insulin after antibody loading give the same peak heights. Therefore, it is possible that there was something wrong with this column. However, the general relationship between the amount of insulin loaded onto the column before and after antibody is loaded remains the same.

Figure 3-5 shows data from 10 μM insulin samples injected onto the same affinity column as the 1 μM samples. Figure 3-5(b) shows an increase in height after reaching a plateau. The reason for this increase is that the antibody bound to the affinity column is starting to become saturated with insulin; this increase is from any excess insulin not bound to the column.

A calibration curve was made from subtraction assay data to determine the linearity of the assay. Figure 3-6 shows a calibration curve from a 4 cm long protein G column which was injected with 5 μL volumes of antibody and insulin solutions. Two injections of blank and insulin were made before antibody was immobilized onto the protein G column. For the blank, peak heights varied by less than 30%. Insulin peak heights varied by less than 10%. The reason for this high variance is not clear. After antibody had been bound to the column, two separate experiments were performed with insulin. For this case, insulin peak heights varied by less than 49% overall. However, for 1 and 5 μM insulin samples the variance between runs was less than 3%. For this experiment the loading and desorbing flow rates were 5 μL/min. These flow rates were chosen to load

and desorb at reasonable times. The protein G column's response to insulin appeared to be linear to 10 μM insulin. Higher concentrations of insulin were not used at this point since the subtraction assay was to determine general binding conditions. The calculated saturation point for the antibody was 23.4 picomoles of insulin; therefore, the response should have been linear to 5 μM insulin. If for some reason, the column was not binding the amount of insulin that it could have, then the apparent saturation point would be higher. This discrepancy in binding capacity was not an issue, since later experiments did not show this high of a difference between theoretical and actual binding capacity.

Loading flow rate characterization. When using a chromatographic preconcentrator, an important characteristic is the speed with which sample can be loaded. If large volume samples are to be preconcentrated, then it is desirable to use high flow rates for sample loading in order to minimize time required for preconcentration. In the case of the protein G system in which antibody is not covalently attached to the surface, each analysis requires two loading steps, one to load antibody and one to load antigen. Therefore, the effect of flow rate on the efficiency of binding for both the antibody and the antigen in the chromatographic system was evaluated.

Table 3-1 illustrates the effect of flow rate on binding antibody to protein G columns. This was evaluated by flowing 20 μL samples of 2.3 μM antibody

Table 3-1: Effect of Loading Flow Rate on Antibody Capture Efficiency.

Flow rate (μL/min)	Percentage of Antibody Captured	Antibody: Mean Peak Height and Std. Dev	Average t_r
1	100	0.2250 ± 0.0049	359.31 ± 5.16
10	98	0.2213 ± 0.0044	293.47 ± 6.29
100	78	0.1763 ± 0.0018	236.75 ± 3.59

through the column at various flow rates. The antibody was desorbed by injection of 20 μL of desorbing buffer at a flow rate of 1 μL/min. The peak height of antibody resulting from the desorption was evaluated at different flow rates shown in the table. (In many cases it has been found that injection of desorbing solutions can prevent accurate quantification in affinity chromatography. Under these experimental conditions, we observed a baseline disturbance associated with the injection of the desorbing solution, however it was well-resolved from the antibody zone thus allowing accurate quantification with these experimental conditions.) As shown, the antibody can be loaded up to 10 μL/min without loss. Even at flow rates of 100 μL/min, 78% of the antibody was captured. It is assumed that the 1 μL/min flow rate captures all of the antibody since lower flow rates were not used. Therefore, the higher flow rate data is calculated as a percentage of the 1 μL/min flow rate. The data for the antibody loading experiment were calculated from five injections of antibody at each flow rate. The average and standard deviation for the peak heights is shown in the table.

After antibody was loaded onto the affinity column, the flow rate was changed to 1 μL/min. To ensure that the flow rate had equilibrated, a five minute waiting time was allowed before desorption was performed. The average retention times (t_r) for the desorbed antibody peak are shown in Table 3-1. There is a great difference between the times for each loading flow rate. This suggests that the actual desorbing flow rate is not 1 μL/min as expected; the flow rate does not equilibrate to the real 1 μL/min flow rate after only five minutes of waiting. There was also a large variation in the t_r between runs. This could cause injection problems when using the on-line system. One injection mode which

could be used is to inject for a short time during the apex of the desorbed peak. The time at which the apex should appear is calculated based on previous experiments. However, with the variation in t_r shown in Table 3-1, the apex of the peak may not appear at the calculated time; therefore, it would be easy to miss the peak entirely and not inject it onto the CZE capillary.

To evaluate the effect of flow rate on binding of insulin to the antibody-loaded protein G support, a subtraction assay was used. To perform the subtraction assay, a 20 µL sample of 0.9 µM insulin in loading buffer was injected onto the column without antibody having been loaded. An identical sample was then injected after the antibody had been loaded. The difference in peak areas resulting from the two injections could be used to determine the amount of insulin that had been captured. The data from this experiment are summarized in Table 3-2. The data illustrate that insulin is effectively captured up to 100 µL/min. One run at each flow rate was performed. The number of moles of insulin injected onto the affinity column should not saturate the column; in fact, the data show that all of the insulin is captured as expected. This indicates that the column used for the subtraction assay discussed earlier was not operating correctly. The volume of the column bed was approximately 0.69 µL, therefore at 100 µL/min the residence time in the column

Table 3-2: Effect of Loading Flow Rate on Insulin Capture Efficiency.

Flow Rate (µL/min)	Percentage of Insulin Captured
5	100
25	100
100	100

was about 414 ms. The fact that all of the insulin was captured at this high flow rate illustrates the rapid binding kinetics possible using this system.

Desorbing flow rate characterization. The volume of the desorbed zone is an important parameter in determining the level of preconcentration that can be achieved. This volume is determined not only by the volume of the packed bed used, but also by the desorbing flow rate. High desorbing flow rates can cause dilution of analyte if desorption is not instantaneous. However, it is also desirable to desorb captured sample from the chromatographic support as rapidly as possible.

The effect of desorption flow rate on the amount of preconcentration was evaluated for the capillary affinity columns. The results are summarized in Figure 3-7. In this experiment, 46.9 picomoles of antibody was loaded onto the column at 10 μL/min. The antibody zone was monitored as it eluted following injection of 20 μL of desorbing solution at various flow rates. Peak height was used for quantification in this case since a concentration sensitive detector was used to compare peaks at different flow rates. With a concentration sensitive detector, the peak area changes as a function of flow rate; but the peak height should remain the same. Therefore in order to compare different flow rates, the peak height is used. For all flow rates, the injection of 20 μL of desorbing solution was sufficient to desorb all of the captured antibody. This was determined by two pieces of evidence. First, a subsequent injection of a desorbing buffer did not produce a new peak. Secondly, it was observed that the peak for the desorbed zone always returned to baseline before the desorbing solution had been completely flushed through the column. As shown, the peak height of the desorbed solutes increases in an exponential fashion with slower flow rates. Thus it is crucial for optimal preconcentration to use low desorbing flow rates.

It was also possible to approximately determine the volume of the desorbed peak by measuring peak width at the baseline and multiplying by the column flow rate. This data is illustrated in Figure 3-8. The increase in dilution at higher desorbing flow rates is due to the relatively slow desorption kinetics. At higher flow rates, much of the mobile phase passes over sorbed solutes before they have time to desorb, therefore a greater volume is required to desorb a given amount of solute. As shown in Figure 3-8, the peak volume at the lowest flow rates used was 1.5 μL. This volume is larger than what can be accommodated by the CZE capillary, therefore some of the sample is inevitably wasted even at a flow rate of 1 μL/min. Typical injection volumes for CZE are on the order of nanoliters. In fact, only 0.1 to 1% of the total peak volume from the affinity column can be used by the CZE separation. Therefore, most of sample from the affinity column is wasted. Although lower flow rates could presumably be used to further decrease dilution and prevent less waste, it was found that the flow system was not as reliable at lower flow rates. However, a different LC pump may be more reliable at lower flow rates.

Characterization of Electrophoresis Conditions

Migration buffer determination. Before it was possible to characterize the coupled chromatographic/electrophoretic system, it was necessary to develop appropriate electrophoresis conditions. The electrophoresis step must resolve antigen from: 1) antibody (since the antibody is desorbed with antigen in the protein G system), 2) non-specifically retained components, and 3) cross-reactive components. Resolution of antibody and antigen is complicated by the fact that they may recombine on the separation column as illustrated in Figure 3-9. For these experiments a tricine buffer at pH 8 was

used as the migration buffer and samples were dissolved in the desorbing buffer. The CZE capillary was bare fused silica. When anti-insulin and insulin were injected separately, they gave reasonable peak shapes and appropriate peak heights. When mixed together and then injected onto the electrophoresis column however, the insulin peak was not observed and the antibody peak tailed noticeably. This suggested that the solutes recombined on the column.

An attempt was made to find a migration buffer that prevented recombination and yielded good peak shapes for both insulin and antibody. Unfortunately, this was not successful. Table 3-3 summarizes the different migration buffers attempted. Insulin was first dissolved in the migration buffer at 1 mg/mL to test the buffer. Then, if the peak shape and efficiency were reasonable, insulin was dissolved in the desorbing buffer. Several buffers gave good results with insulin, but poor results with a mixture of antibody and insulin.

The best separation was obtained when the desorbing solution was used as the migration buffer. With this migration buffer, it was necessary to use a capillary that had an inner surface modified to contain positive charges to repel proteins which were positively charged at the low pH. Polybrene coating was used for this purpose. Using this migration buffer and column coating, the insulin peak shape and area was unaffected by the presence of antibody in solution as shown in Figure 3-10. It was concluded that the new migration buffer effectively prevented recombination of insulin and antibody on the column. These separation conditions also yielded a reasonably efficient insulin zone, however the efficiency of the antibody zone was low. Thus, these separation conditions are a

Table 3-3 Migration Buffers For CZE.

Migration buffer	Capillary i.d. (μm)	Buffer of Insulin Solution	Injection	CZE Voltage	N
0.85 M CHES, 0.05 M sodium acetate pH 7.8 with 10% CH_3CN	50	migration buffer	30 s, gravity	25 kV	46,000
0.85 M CHES, 0.05 M sodium acetate pH 7.8 with 10% CH_3CN	50	0.05 M NaH_2SO_4, 0.05 M K_2SO_4 pH 3	10 s, 5 kV	25 kV	46,300
10 mM tricine, 0.1 M K_2SO_4 pH 10	25	migration buffer	5 s, 3 kV	20 kV	29,700
10 mM tricine, 0.1 M K_2SO_4 pH 10	25	0.1 M glycine, 0.05 M K_2SO_4, 20% CH_3COOH	5 s, 5 kV	20 kV	4,600
10 mM tricine,0.1 M K_2SO_4 pH 8.3	25	migration buffer	10 s, 10 kV	20 kV	6,400
0.1 M tricine, 0.05 M K_2SO_4 pH 8.03	25	migration buffer	5 s, 5 kV	20 kV	21,200
0.1 M tricine, 0.05 M K_2SO_4 pH 8.03	25	migration buffer	5 s, 5 kV	20 kV	13,000
0.2 M glycine, 0.05 M K_2SO_4 pH 10	25	migration buffer	5 s, 5 kV	20 kV	6,000
0.1 M glycine, 0.05 NaH_2PO_4, 10% CH_3COOH pH 3 (polybrene coated)	25	0.05 M NaH_2SO_4, 0.05 M K_2SO_4 pH 3	60 s, gravity	25 kV	73,000
0.05 M NaH_2PO_4 pH 3 (polybrene coated)	25	migration buffer	15 s, gravity	25 kV	7500
0.05 M NaH_2PO_4 pH 3 (polybrene coated)	25	0.1 M glycine, 0.05 M K_2SO_4, 20% CH_3COOH	30 s, gravity	25 kV	9,200
0.1 M glycine, 0.14 M H_3PO_4 pH 3 (polybrene coated)	25	0.05 M NaH_2SO_4, 0.05 M K_2SO_4 pH 3	10 s, 5 kV	29 kV	4200
0.1 M glycine, 0.14 M H_3PO_4 pH 3 (polybrene coated)	25	migration buffer	10 s, 10 kV	29 kV	12,400

compromise, but yield a useful signal for the analyte antigen. It is not clear whether the breadth of the antibody zone was due to partial resolution of microheterogeneity of the antibody or whether it was due to adsorption.

Internal standard selection. For off-line affinity chromatography and CZE, it was important that an internal standard be used. The injection method for the off-line system was performed hydrodynamically; therefore, an internal standard would compensate for any variations in injection volume. Table 3-4 summarizes the internal standards tried.

Table 3-4: Internal Standard Selection.

Attempted Internal Standard	Results
Dopamine	t_m longer than insulin and antibody
Sodium azide	more than one peak
3,4-dihydroxyphenylacetic acid	peaks disappeared over time
Phenol	peak at same time as a "dip" in the baseline
Ascorbic acid	acceptable

The internal standard which was determined to work best in our system was ascorbic acid.

Interface optimization. In order to perform on-line affinity chromatography and CZE, an interface joining the two capillaries was necessary. Figure 3-11 shows the interface in detail. The outlet of the affinity column and the inlet of the CZE capillary are positioned directly opposite each other. For optimum injections, it is important that the two capillaries are as close as possible. When the CZE voltage is applied during a run, buffer is swept into the capillary. If the capillaries are too close together, then the effluent from the affinity column will be injected continuously into the CZE column. Therefore, before injection of a real sample, an unretained solute was injected onto the affinity column and the capillary distance was optimized. To do this, the junction capillary which connected the affinity column to the interface was held stationary while the CZE capillary was manipulated. The first distance used was when the two capillaries were flush against

each other. Then, the CZE capillary was moved away from the junction capillary until no effluent entered the CZE capillary during a CZE run. The CZE capillary was marked at 3 cm from the inlet; when the screw holding the capillary in place was tightened, this mark was 2-3 mm from the edge of the screw. Whenever a new CZE capillary was used, the optimization step started with the 3 cm mark; if the CZE capillary needed to be manipulated further, it was only 1 or 2 mm.

The flow rate of the gating flow was also an important variable. The gating flow needed to be fast enough to make sure that the effluent from the affinity column did not enter the CZE capillary, especially during the antibody loading step. Experiments were performed using the highest flow rates expected to be used for the affinity column and then varying the gating flow rate. It was found that a flow rate of 2 mL/min or greater was needed to rinse all of the effluent away during loading of the antibody.

Protein G - Noncovalent Coupled with CZE

Concentration calibration. An example of a calibration curve based on different concentrations of insulin for the affinity system combined off-line with CZE is shown in Figure 3-12. In this experiment, 500 μL samples of insulin were injected onto the affinity column at 100 μL/min, desorbed with a 500 μL injection of desorbing solution at 5 μL/min, and a 5 μL fraction expected to contain the insulin/antibody peak was collected. An internal standard, ascorbic acid, was added to the collected fraction prior to injection onto the CZE to account for injection volume errors so the peak area for insulin is plotted as the ratio to the ascorbic acid peak. The protein G column had been loaded with 58.6 picomoles of anti-insulin. The calibration curve shows the peak area ratio observed in the

electropherogram versus the concentration injected onto the affinity column. As shown, a linear relationship is observed up to an injection of 225 nM (112 picomoles based on a 500 μL injection volume) onto the affinity column. This is in agreement with the expected results since 58.6 picomoles of anti-insulin had been loaded onto the column and each mole of antibody is expected to bind two moles of antigen (assuming that steric hindrance does not prevent full loading of the antibodies) for an expected binding capacity for the affinity column of 117 picomoles. Each point is the average of 2 runs and the duplicate runs varied by an average of 9.2%.

The preconcentrated peak areas for insulin agreed well with peak areas for insulin samples which were injected directly onto the CZE column at concentrations expected following preconcentration as shown in Figure 3-12. In other words, 500 μL volumes were injected onto the chromatography column and the peaks were collected in a 5 μL volume for a 100-fold preconcentration. Therefore, a fraction collected from an injection of a 115 nM sample should give the same peak area in the CZE separation as the direct injection of a 11.5 μM sample onto the CZE. Although the slopes of the two lines are slightly different, it is apparent that good agreement is observed up to the point of saturation of the affinity column. Thus, the system allows quantitative, predictable preconcentration.

For the experiments depicted in Figure 3-12, non-zero intercepts were consistently observed. It is not clear what caused this effect; however loss of insulin due to recombination with the antibody or to adsorption to the capillary wall is a likely explanation.

An example of calibration for the on-line system is shown in Figure 3-13. In this case, 20 μL of sample was loaded at 10 μL/min. There was no need to use higher flow rates than 10 μL/min as the sample size was relatively small. Desorption was performed by injection of 20 μL of desorbing buffer at 5 μL/min. Although 1 μL/min would have given better preconcentration, a desorbing rate of 5 μL/min was used. At a flow rate of 5 μL/min, there seemed to be less of a variance between runs than at 1 μL/min after changing the flow rate. Each point represents the average of two injections. Duplicate runs varied by an average of 12.4 %. As with the off-line injection, a linear relationship is apparent up to the expected point of saturation of the affinity column. The column had been modified with 46.9 picomoles of antibody (93.8 picomoles binding capacity) and the curve becomes non-linear between 100 and 160 picomoles of insulin injected.

A problem with performing on-line injections is capturing the desorbed zones reproducibly. The best preconcentration would be obtained by a brief CZE injection exactly as the apex of the desorbed antigen/antibody zone eluted from the affinity column. Unfortunately, with this strategy small changes in chromatographic retention time lead to large changes in the concentration injected onto the CZE column and poor reproducibility. Therefore, for these preconcentration studies, the CZE injections were 60 s long. The time for injection was chosen so that the middle of the injection coincided with the expected apex of the eluting antigen/antibody zone. The long injection time increased the chance that the zone would elute during the injection time and be reproducibly represented in the injection volume. The drawback is that during most of the injection time, the less concentrated portions of the zone would be at the inlet of the CZE and be injected.

Several possibilities exist for improving the preconcentration effect. One would be to add a second detector at the exit of the affinity column. This detector would allow the exact elution time of the antibody/antigen zone to be determined and could be used to trigger injection onto the CZE column at the correct time.

Volume calibration. It is also of interest to determine the effect of sample volume on the preconcentration effect. An example of a volume calibration curve is shown in Figure 3-14. This experiment was performed in a fashion similar to the off-line concentration calibration except that a 25 nM insulin solution was loaded at 100 μL/min and the injection volume was varied from 0.5 to 2.0 mL. The desorbed insulin/antibody zones were collected in 1 μL fractions and diluted to 5 μL with desorbing solution containing 0.2 mM ascorbic acid as an internal standard. The figure illustrates that a linear relationship is observed with increasing injection volume.

The areas of preconcentrated insulin zones agree well with direct injections of insulin at the expected concentrations after preconcentration up to about 1 mL of sample. The failure above 1 mL does not appear to be due to saturation of the affinity column. For example, a 1.5 mL injection of 25 nM insulin contains 38 pmol of insulin yet the column was loaded with 47 pmol of antibody which should bind up to 94 pmol of insulin. In addition, larger mass samples were loaded onto the affinity column in the experiment depicted in Figure 3-12 without saturation. Rather it seems that the insulin was not bound tightly enough to the antibody to be retained for the time required to flow samples greater that 1 mL through the column. Thus, some insulin was lost during sample loading. This loss of antigen may be due to the relatively poor binding constant of the antibody to the

antigen (5×10^7 L/mol). Better binding antibodies would be expected to have slower dissociation rate constants and have lower losses during loading. While the amount of preconcentration is not as great as expected at sample volumes over 1 mL, the linear relationship means that it is possible to perform preconcentration with samples that large. The desorbed peak volume was 1 μL for this column; therefore, the total preconcentration achieved for the 1 mL sample is 1000-fold. Since the desorbed peak was diluted by a factor of five through the addition of internal standard, the measured preconcentration was 200-fold.

Selective preconcentration. Electropherograms showing a high level of preconcentration are shown in Figure 3-15. The upper trace illustrates an electropherogram originating from an injection of 1.0 mL of 25 nM insulin onto the affinity column. The lower trace is a direct injection of 500 nM insulin onto the CZE column. Clearly the preconcentration achieved allows a much lower detection limit. For example, the detection limit for insulin using the off-line system, a 1 mL injection volume, and a five-fold dilution with internal standard after fraction collection was approximately 9 nM. Better detection limits are possible if the sample is not diluted after fraction collection. By comparison, the detection limit for insulin by direct injection onto the same CZE system was 2 μM. Detection limits were determined as the concentration that gave a peak height two times the peak to peak noise.

The importance of selectivity in preconcentration is shown in Figure 3-16. In Figure 3-16(a), a 10-fold dilution of serum sample spiked with 175 nM insulin was injected onto the electrophoresis column. The electrophoresis conditions are clearly not optimized for a

serum sample, however it is apparent that it would be difficult resolve insulin from large zones associated with immunoglobulins, albumin and other highly concentrated proteins found in serum. Figure 3-16(b) is an electropherogram after 500 μL of the same sample had been preconcentrated using the combined system. The effective clean-up afforded by the immunoaffinity column allows the insulin zone to be clearly identified. In this electropherogram, it appears that the antibody zone is starting to overlap the insulin zone. In fact, the overlap is only apparent when using serum samples. This suggests that the overlap is probably due to components of the serum sample which were desorbed with insulin. This could be non-specifically adsorbed proteins or immunoglobulins which were bound by the protein G support. The ability to discriminate against adsorption of components other than antigens illustrates one of the advantages of using a second separation dimension with immunoaffinity chromatography.

Insulin in serum samples was preconcentrated to only about 50% of the expected value. These results indicate that the large number of components in serum which may non-specifically adsorb to the affinity column may effectively compete for binding to the antibody under the conditions used here. It is also possible that the immunoglobulins in the serum sample displace the insulin antibody from the protein G support causing sample loss. Quantitative work in complex samples will require calibration methods that account for this possibility.

Characterization of Epoxide Activated Columns

There are several advantages to using affinity columns with antibody covalently attached to the chromatographic support. First, less harsh desorbing buffers could be used

than with noncovalently attached antibody. Second, the second separation step using CZE will be greatly simplified without the antibody peak. Finally, the total time for analysis will be shorter since there is no need to reload the column with antibody after every run. However, the ability to change the antibody after each run is traded for selectivity of the column. Perfused particles activated with epoxide groups were the first chromatographic support tested.

Loading flow rate characterization. As with protein G columns, the epoxide activated columns were tested to determine the effect of flow rate on insulin binding. Figure 3-17 shows the data from this study. In this case 20 μL of 100 nM insulin in loading buffer was injected onto the column at various flow rates. Insulin was desorbed from the column at a flow rate of 1 μL/min. When the desorbed peak areas were compared, the low and high flow rates show similar values. Therefore, flow rates up to 75 μL/min should bind all insulin which was injected onto the column. Chromatograms of 100 nM insulin and a blank loaded at 5 μL/min are shown in Figure 3-18. Figure 3-19 shows the desorbed insulin peak and a blank. The large decrease in the baseline is due to the absorbance of the desorbing buffer being slightly different from that of the loading buffer. A desorbing flow rate study was not performed with the epoxide activated particles since the previous study with protein G columns indicated that a slower flow rate was better. A flow rate of 1 μL/min was used to desorb the insulin during further experimentation.

Calibration and capacity of column. Before the calibration was done, the capacity of the column to bind insulin was determined. A breakthrough curve (figure 3-20) was

determined from injecting 20 μL of 500 nM insulin at a flow rate of 10 μL/min; this breakthrough curve determines the saturation point of insulin binding to the column. The number of moles of insulin bound to the column was calculated from the time it took the 500 nM insulin to start overloading the column. This overload time was 90 s and the number of moles of insulin bound by the antibody was 7.5 picomoles.

A calibration curve was performed on a 3.5 cm long column using 5 μL/min flow rates for both loading and desorbing. Figure 3-21 shows the results of this experiment. The curve reaches a saturation level at 500 nM, and all concentrations greater than that give the same peak area. Another type of calibration curve was also performed. In this second type, increasing volumes of the same concentration are injected onto the column to obtain a calibration curve. Figure 3-22 shows the calibration performed using 50 nM insulin with increasing volumes up to 100 μL injected onto the column. The insulin solution was loaded onto the epoxide activated column at a flow rate of 50 μL/min and then desorbed at 1 μL/min. Figure 3-22 shows that the data is linear for the volumes tested. Volumes greater than 100 μL were not injected because the saturation point was calculated to be 150 μL; therefore, this data was expected to be linear.

Further experiments were not performed using the epoxide activated covalent columns because of their low capacity as compared with the protein G columns. For the data shown in Figure 3-22, the capacity of the packing material to bind antibody was 0.87 mg/mL. This value was obtained from the number of moles of insulin bound during the breakthrough curve experiment. With this small capacity, the number of moles of insulin bound was too small to detect on the CZE with UV-VIS detection. It may be possible to

increase the number of moles of antibody bound to the epoxide activated support by changing the binding conditions. However, since the protein G particles had an antibody binding capacity of 10-20 mg/mL and the antibody could be bound covalently to the support by a cross-linker, these protein G covalent columns were explored instead of continuing with the epoxide activated columns.

Characterization of Protein G Covalent Columns

Protein G columns with antibody covalently attached through a cross-linker were the second type of covalent columns tested. Experiments were performed in order to characterize this type of column although it was expected that the behavior would be similar to protein G columns with antibody noncovalently attached.

Insulin response. In order to determine if any antibody was actually covalently attached to the column, a calibration curve using 10 μL/min flow rates for loading and desorbing was performed. A 20 μL injection loop was used to inject sample onto the column; therefore, a 10 μL/min flow rate was used in order to perform the experiment quickly. A calibration curve for a 10.5 cm long column loaded with 20 μL of 2.3 μM antibody is shown in Figure 3-23. The column responded to insulin in a manner similar to protein G noncovalent. The insulin response was linear until 5 μM with a correlation coefficient of 0.977 and the saturation of the column occurred between 5 and 10 μM. The theoretical saturation point of the antibody for insulin was calculated to be 11.6 μM when 20 μL are injected.

Characterization of loading flow rate. Although the non-covalent protein G columns had already been characterized, the covalent protein G columns needed to be studied in

case they performed differently. Therefore, a loading flow rate study using a 9.3 cm long column with 102.7 picomoles antibody immobilized was performed. A concentration of 5 μM insulin was loaded at various flow rates and then desorbed from the column at 5 μL/min. Figure 3-24 shows a chromatogram during the loading of 5 μM insulin onto the affinity column. The baseline drift was not important for quantitation because this peak was not used to calculate the response to the flow rate. An example of a chromatogram from the desorbing step for a covalent protein G column is shown in Figure 3-25. Figure 3-25(a) shows the desorbed insulin peak while (b) shows the desorption buffer. Figure 3-26 shows that a loading flow rate up to 100 μL/min is reasonable without loss of insulin. Three samples at each flow rate were used and their average was plotted in Figure 3-26.

Characterization of desorbing flow rate. To determine whether the covalent protein G columns performed in the same manner as noncovalent protein G for desorption, variable flow rates were used to desorb insulin from a 10.1 cm column. Only flow rates up to 8 were tried, as previous experience showed that anything higher would not be desirable. Figure 3-27 shows that the protein G covalent columns do in fact show a response similar to protein G non-covalent columns. The best desorbing flow rate was again near 1 μL/min but the peak height decreased by half from 1 to 8 μL/min. Although the best desorbing flow rate was 1 μL/min, there was still the problem with the LC pump equilibrating at this flow rate. Therefore, desorbing flow rates used were 5-10 μL/min.

Protein G covalent coupled with CZE. Protein G covalent columns were used for an on-line calibration. In this experiment, a covalent column was used which had 46.9 picomoles of antibody bound to it. Volumes of 20 μL of insulin in loading buffer were

injected at 10 μL/min. After the desorbing buffer was rinsed through the column, a 40 s injection at 5 kV was used to inject insulin onto the CZE capillary. The CZE capillary had a 25 μm i.d. and a 10 cm injector to detector length. An example of an electropherogram of 2 μM insulin for this system is shown in Figure 3-28. The dips shown in the electropherogram result from the desorbing buffer. With this large baseline disturbance, it may be difficult to use this system with other analytes if their migration time is the same as the disturbance. Figure 3-29 shows the calibration curve using the coupled system. Three to four runs were averaged for each point. Relative standard deviations not greater than 21% were observed. It is not clear why the reproducibilty was not very good. As in the case of the calibration curve for protein G noncovalent coupled with CZE, a linear response for the calibration curve is observed. As was similar with protein G non-covalent, a non-zero intercept was observed for the covalent column.

Concluding Remarks

Protein G immunoaffinity chromatography allows extensive and selective preconcentration of analytes from complex mixtures for CZE analysis. The high flow rates possible with the system facilitate reasonable analysis times. For example, a 1 mL sample can be loaded onto an affinity column in 10 minutes using a 100 μL/min flow rate. The use of separate columns for preconcentration and electrophoresis provides several advantages including protection of the electrophoresis column and no loss of CZE separation efficiency because of slow desorbing kinetics. The method of coupling at present does not utilize a large part of sample even though large gains in analyte concentration can be obtained.

The combination of capillary immunoaffinity chromatography and CZE should have many applications besides preconcentration and clean-up of samples for electrophoresis. This system is a microscale, electrophoretic analog of dual-column immunoassays in which an immunoaffinity column is coupled to a liquid chromatography column (15-17, 60-62). These systems are highly versatile and have been used to determine not only antigens (60), as was done here, but also antibody titers (16), and protein variants (17). Immunoaffinity chromatography has also been used to remove highly concentrated components from a sample, such as albumin from serum, to simplify the second chromatographic separation (4). Applications such as these should be possible on this dual column system with the added advantages associated with using capillary electrophoresis in the second dimension.

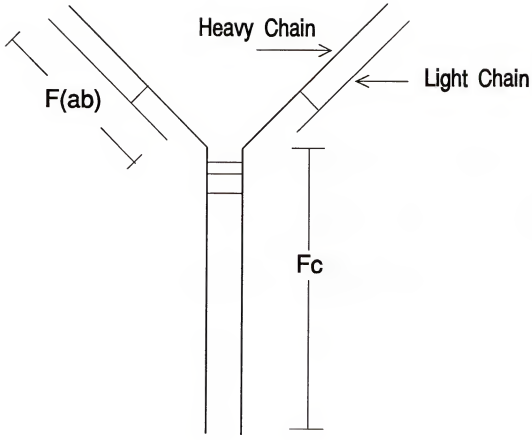

Figure 3-1. Schematic of the type of antibody used in this work.

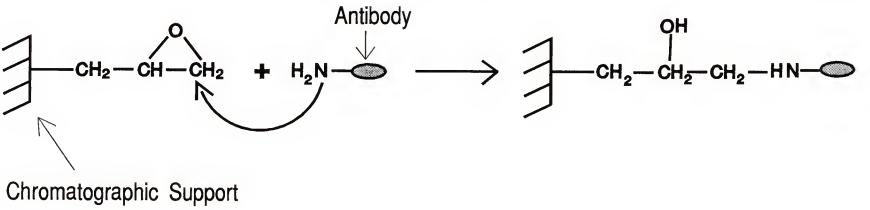

Figure 3-2. Reaction of antibody with epoxide activated support.

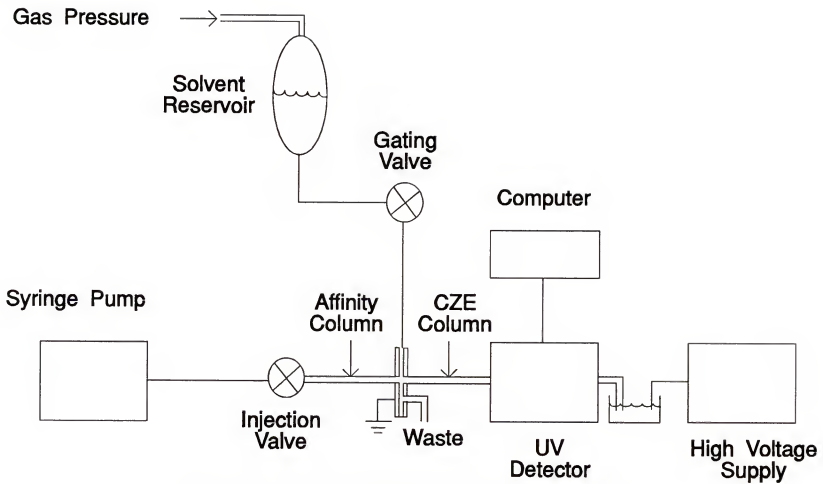

Figure 3-3. Schematic of liquid chromatography coupled with CZE.

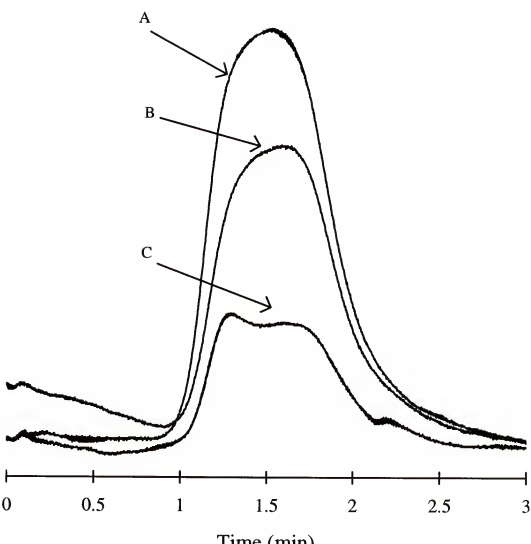

Figure 3-4. Subtraction assay using 1 μM insulin. Chromatograms showing (A) insulin loaded onto a protein G column (B) insulin loaded onto a protein G column with antibody immobilized (C) a blank loaded onto the same column.

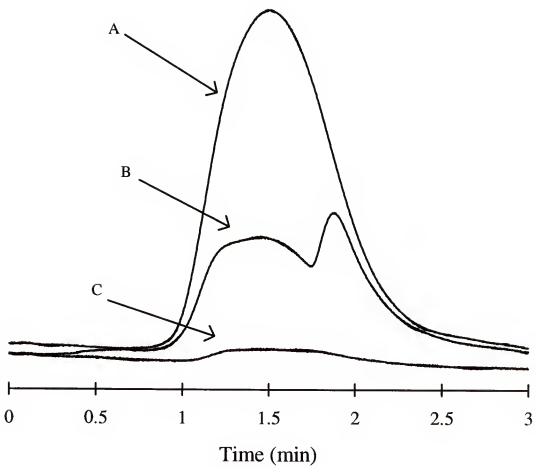

Figure 3-5. Subtraction assay with 10 μM insulin. (A) Chromatogram of 10 μM insulin loaded onto a protein G column. (B) Chromatogram of 10 μM insulin loaded onto a protein G column immobilized with antibody. (C) Chromatogram of a blank loaded onto the protein G column.

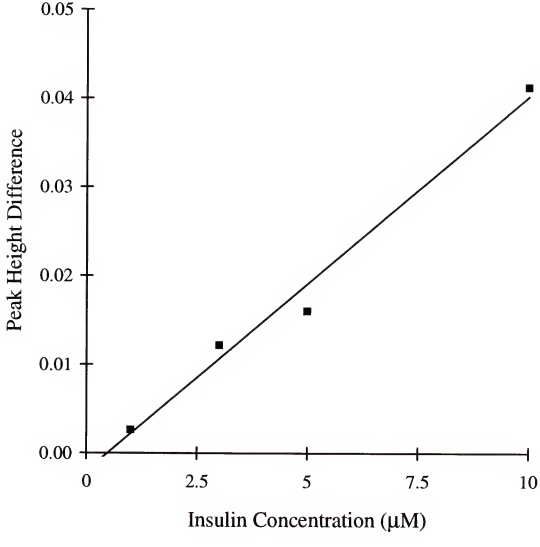

Figure 3-6. Peak height difference as a function of insulin concentration showing the results of a subtraction assay.

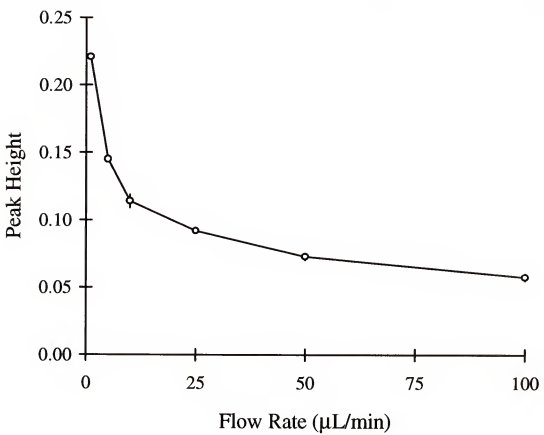

Figure 3-7. Effect of desorption flow rate on antibody response.

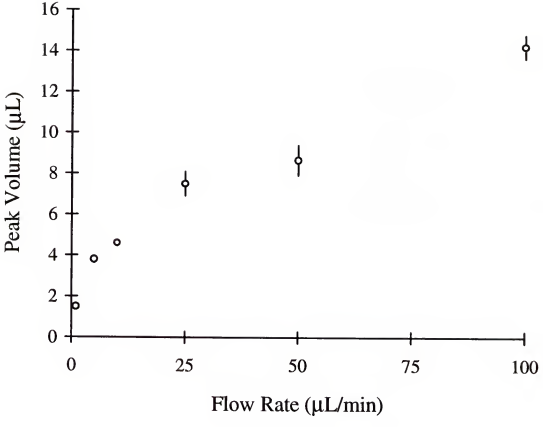

Figure 3-8. Peak volume as a function of flow rate shows the effect of desorption flow rate on preconcentration. Points are the average of duplicate runs with error bars showing the range of values.

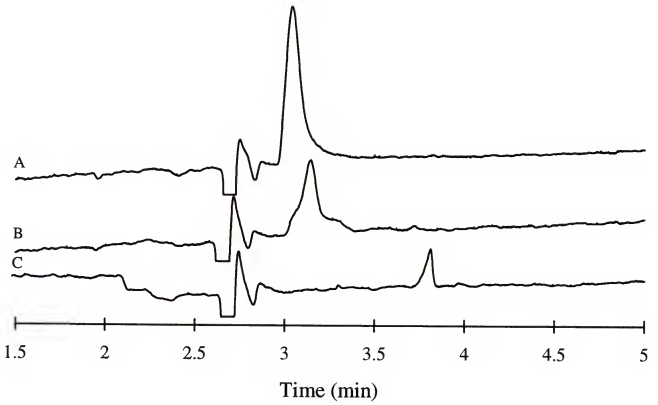

Figure 3-9. Electropherograms of (A) 9 μM anti-insulin, (B) a mixture of 20 μM insulin and 9 μM anti-insulin, and (C) 20 μM insulin. All samples were dissolved in desorbing buffer and injected hydrodynamically. The migration buffer was 0.1 M tricine, 0.05 M K_2SO_4 pH 8. The CZE capillary was uncoated fused silica.

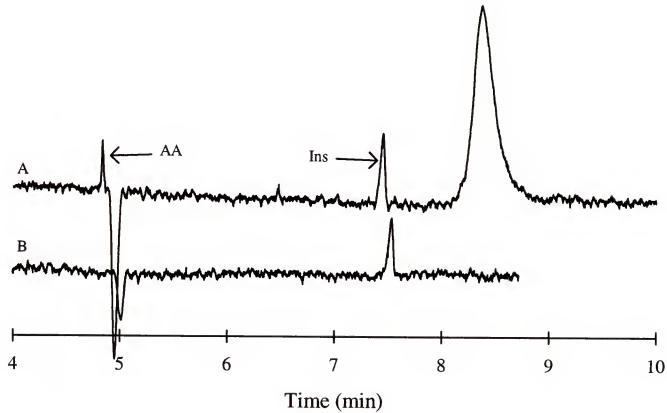

Figure 3-10. (A) Electropherogram of a mixture of 20 μM insulin and 9 μM anti-insulin using desorbing solution as migration buffer. (B) Electropherogram of 20 μM insulin under the same conditions. All other CZE conditions are same as for off-line combination given in Experimental section.

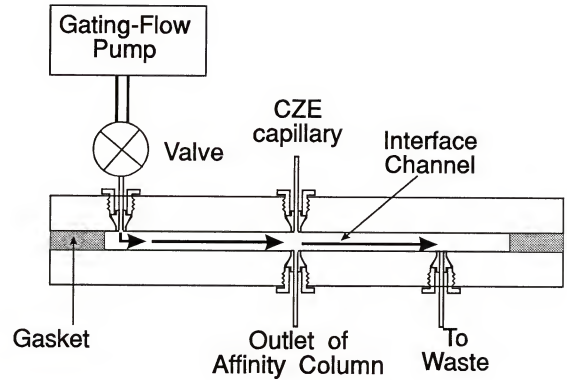

Figure 3-11. Schematic of the gating flow interface used to connect the chromatography column with the CZE column.

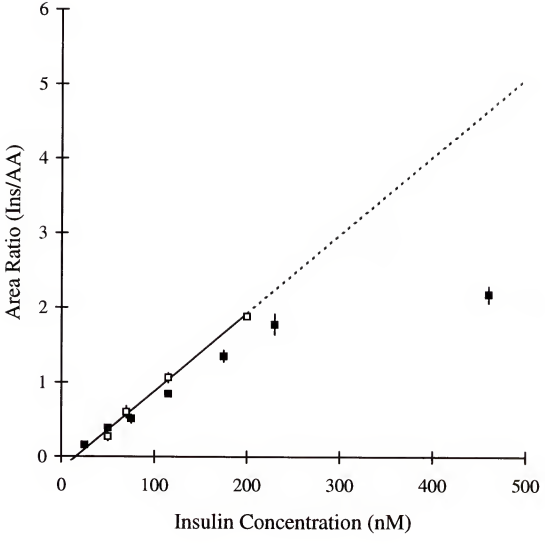

Figure 3-12. Calibration curve for an affinity column coupled off-line with CZE for preconcentrated insulin samples (■) and standards (□). The line corresponds to the best fit line for the standards. The standards were injected onto the CZE column at concentrations that corresponded to that expected following a preconcentration of the concentration given on the x-axis. Points are the average of duplicate runs with error bars showing the range.

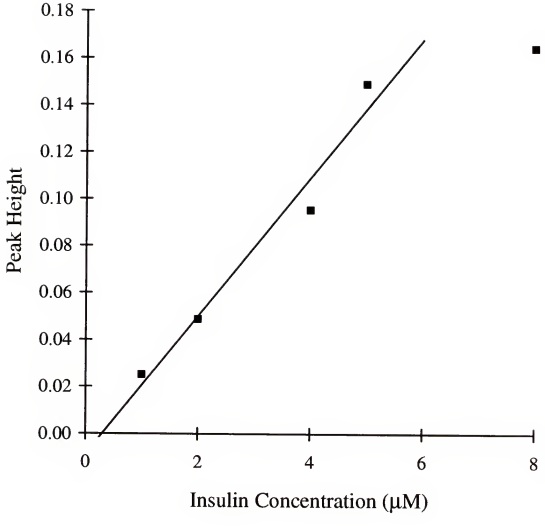

Figure 3-13. Calibration curve for on-line coupling of affinity column with CZE. Peak height is that observed in the electropherogram and the insulin concentration is the concentration injected onto the affinity column. The line is the linear regression best fit to the linear portion of the curve.

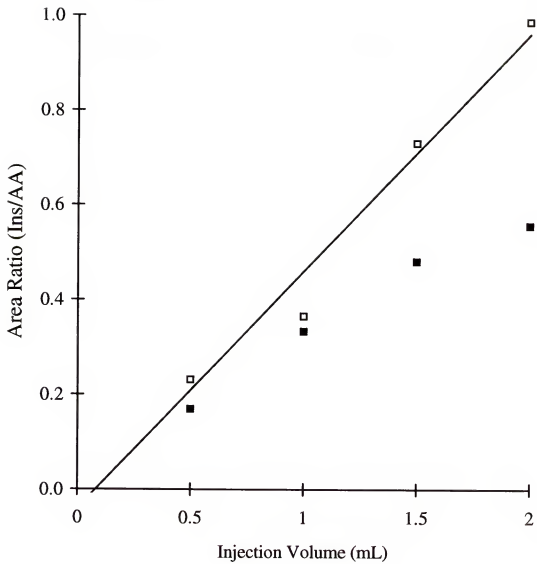

Figure 3-14. Injection volume calibration curve for off-line coupling of affinity column to CZE. (■) are the preconcentrated samples. (□) are standards injected at the concentrations expected following preconcentration from the volume on the x-axis. The line corresponds to the best fit line for the standards.

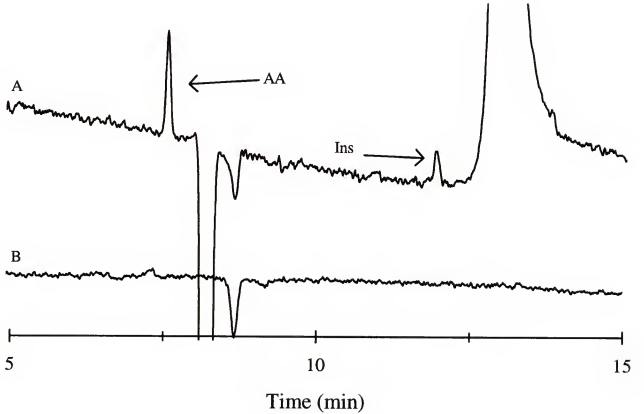

Figure 3-15. Preconcentration of 25 nM insulin using off-line system. (A) Electropherogram of 1 mL of 25 nM insulin preconcentrated to 5 μL. AA indicates the ascorbic acid internal standard and Ins indicates the insulin zone. The large zone to the right of the insulin zone is the desorbed antibody. (B) Electropherogram of 500 nM insulin injected directly onto CZE.

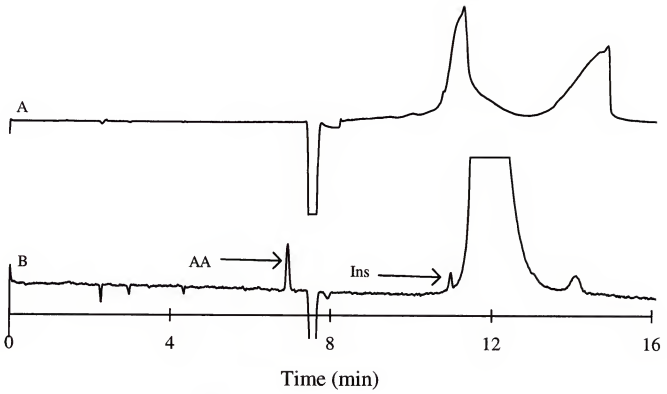

Figure 3-16. (A) Electropherogram of bovine serum sample spiked with 175 nM insulin injected directly onto CZE. (B) Electropherogram of same sample after preconcentration with the affinity column. Sample preparation procedures and electrophoresis conditions given in text. 10-fold higher gain was used in the preconcentrated electropherogram.

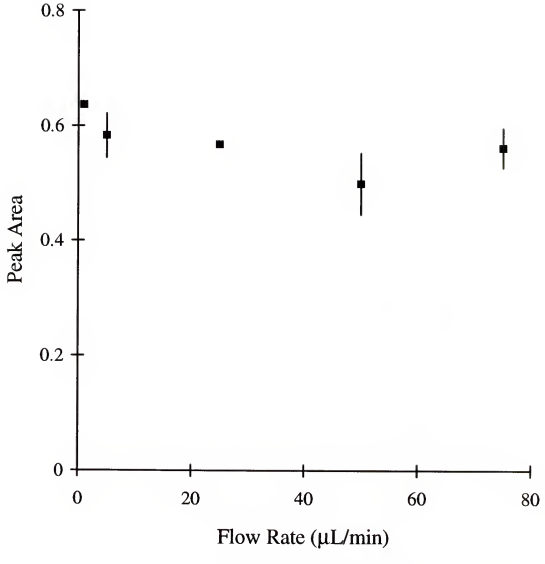

Figure 3-17. Effect of loading flow rate on peak area of desorbed insulin. Points are averages of duplicate runs with error bars showing the range of values.

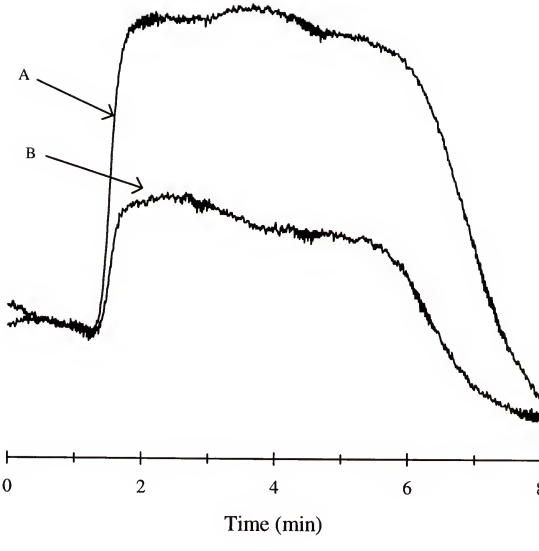

Figure 3-18. Chromatograms of (A) 100 nM insulin and (B) a blank loaded onto an epoxide activated column.

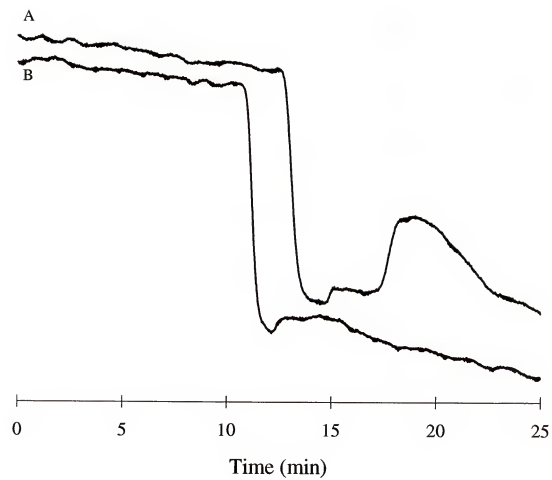

Figure 3-19. Chromatograms showing desorbed peaks from an epoxide activated column. (A) 100 nM insulin desorbed at 1 μL/min. (B) Desorbing buffer injected onto the column at 1 μL/min flow rate.

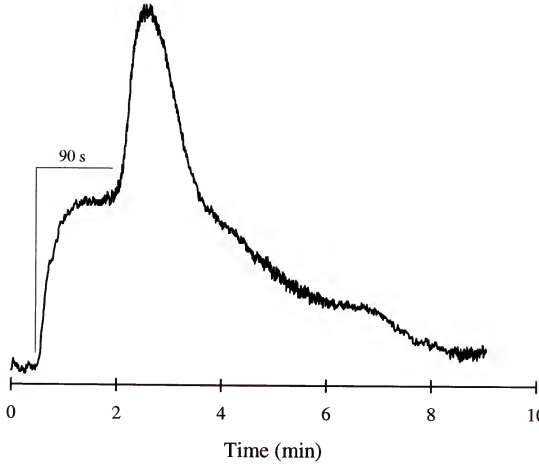

Figure 3-20. A 500 nM insulin breakthrough curve for a 3.5 cm long epoxide activatd column. The 90 s time interval is the breakthrough time.

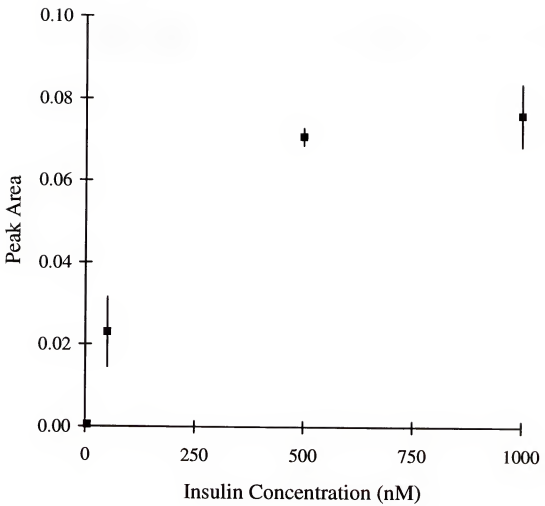

Figure 3-21. Calibration curve for an epoxide-activated column. Points are the average of 3 runs with error bars showing the range of values.

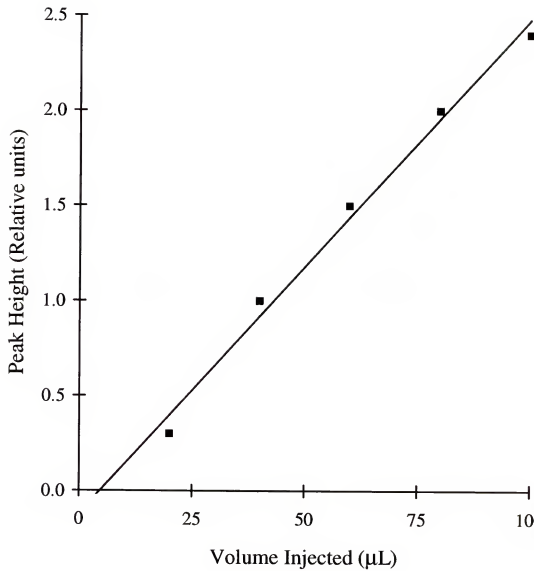

Figure 3-22. Calibration curve for an epoxide activated column using 50 nM insulin injected at different volumes. The line through the points represents the best fit line based on linear regression.

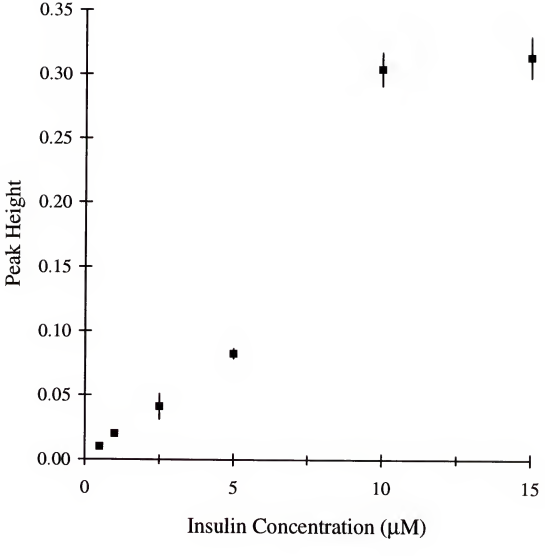

Figure 3-23. Calibration curve for a protein G column with antibody covalently bound. Points are averages of duplicate runs with error bars showing the range of values.

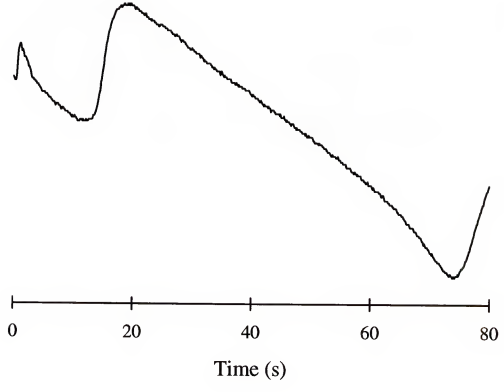

Figure 3-24. Chromatogram of 5 μM insulin during loading of insulin onto the protein G covalent column.

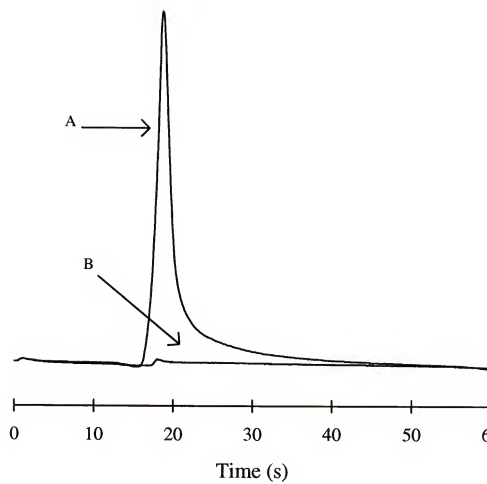

Figure 3-25. (A) Chromatogram of 5 μM insulin during desorption from the protein G covalent affinity column. (B) Chromatogram of desorbing buffer injected onto the protein G covalent column.

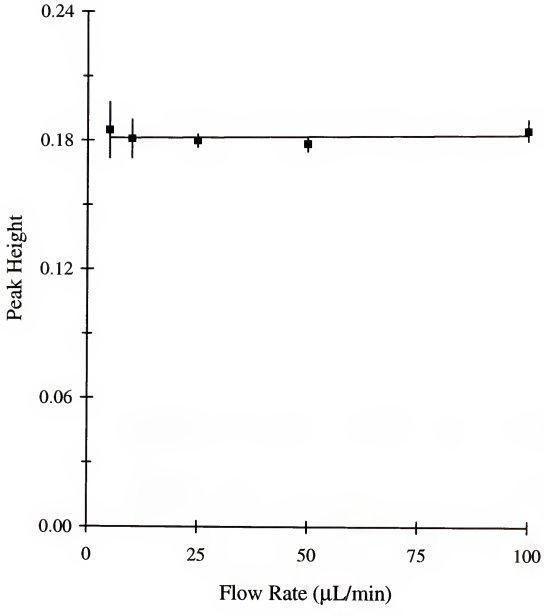

Figure 3-26. Effect of loading flow rate on desorbed insulin for a protein G column with antibody bound covalently. Points are averages of duplicate runs with error bars showing the range of values.

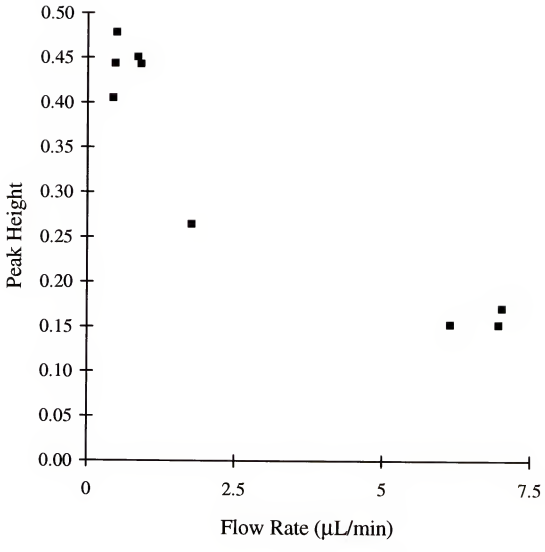

Figure 3-27. Effect of desorbing flow rate on desorbed insulin peak height with antibody bound covalently.

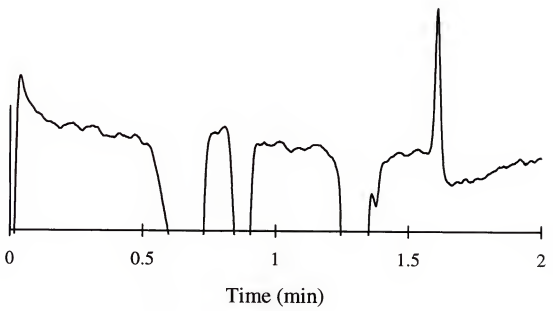

Figure 3-28. Electropherogram of 2 μM insulin using a protein G covalent chromatography column coupled on-line with CZE.

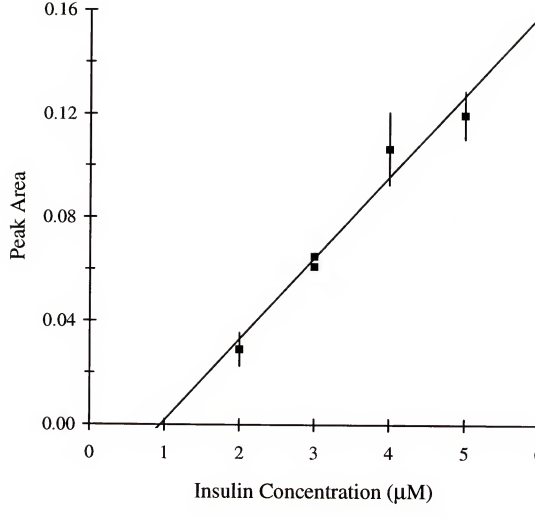

Figure 3-29. Calibration curve for a protein G with antibody bound covalently coupled on-line with CZE for preconcentration of insulin samples. The line corresponds to the best fit line for the samples. The points with error bars were averaged from 3 runs with error bars showing the range of values.

CHAPTER 4
EPITOPE MAPPING

Introduction

Epitope mapping is the process of determining the specific region of an antigen that an antibody recognizes. Determination of epitopes is a fundamental step in developing an understanding of the antibody-antigen interaction. Such knowledge is of interest in many areas of study including autoimmune diseases (63, 64), immunodiagnostics (65), protein characterization (66,67), drug design, and the mechanism of antigen-antibody binding (68). There are two types of epitopes: linear and discontinuous. In a linear epitope, the binding region is composed of a continuous sequence of amino acids. However, in a discontinuous epitope, the binding region is composed of amino acids which are close due to the 3-D structure of the polypeptide, but are far apart in sequence.

Several techniques have been used to determine epitopes. One method which can be used is peptide synthesis of overlapping peptides of the antigen (69-72). For example, these peptides can be synthesized on polyethylene pins (71) and polypropylene membranes (72). Once the peptides are synthesized, they are tested for binding to the antibody of interest. After identification of peptides which bind to the antibody has been accomplished, further testing can be performed by making all of the single amino acid substitutions for the binding peptides. In this manner, single amino acid resolution has been achieved (71).

Another method uses an epitope library composed of fusion phages to determine epitopes (73). A fusion phage is a bacteriophage vector which has foreign amino acid sequences inserted into the vector. The amino acid sequence is displayed on the surface of the fusion phage and any phages with possible epitope regions can be selected from non-epitope carrying phages by affinity purification. Advantages of this method are: 1) phages can be cloned to provide large numbers of the possible epitope regions, 2) ligands for antibodies with unknown antigens can be identified, and 3) potential use in determining discontinuous epitopes.

Recently, mass spectrometry has seen use in epitope mapping (74-76). One method which uses mass spectrometry (MS) to identify digested regions of an antigen which is bound to the antibody has been performed (75). In this case, the antigen was bound to an immobilized antibody before digestion with trypsin. The digestion process does not harm the antibody/antigen binding region. Mass spectra were obtained for the digestions of free antigen and antigen bound to antibody. The non-binding peptide digests were analyzed and once they were removed from the antibody/antigen complex, the bound peptide region was dissociated from the antibody and analyzed. This method can be used before one of the other processes mentioned earlier in order to simplify the process.

Mass spectrometry has been used in another manner to accomplish epitope mapping. For this case, antigen is digested and then the epitope region is immunoprecipitated from the non-epitope regions with monoclonal antibody attached to beads (76). This method utilizes matrix assisted laser desorption ionization time of flight mass spectrometry (MALDI-TOFMS) to identify the peptide fragments which bound to the antibody.

The goal of the work presented in this chapter was to explore the use of immunoaffinity chromatography and capillary electrophoresis in combination with MALDI-TOFMS for linear epitope mapping. A capillary immunoaffinity column was used to selectively bind epitope fragments produced from digestion of whole antigen with trypsin, α-chymotrypsin and clostripain or pepsin. Capillary zone electrophoresis (CZE) and MALDI-TOFMS were used to characterize the whole digests, bound portion of the digests, and unbound portion of the digests. The system was tested on insulin and a fragment of glucagon like peptide-1 (GLP-1 7-36).

Experimental

Chemicals and materials. Tricine and sodium azide were obtained from Aldrich Chemical Co. (Milwaukee, WI). Calcium chloride, potassium sulfate, and sodium phosphate were obtained from Fisher Scientific (Pittsburgh, PA). α-Chymotrypsin, trypsin, clostripain, pepsin, DL-dithiothreitol, oxidized B-chain of bovine insulin, bovine insulin, GLP-1 7-36 were from Sigma Chemical Co. (St. Louis, MO). Human insulin (Humulin R) was from Eli Lilly and Company (Indianapolis, IN). Anti-insulin C-terminal pentapeptide clone #C7C9 was from Biodesign International (Kennebunk, ME). Anti-GLP-1 7-37 No. 26.1 mouse monoclonal antibody was from Dr. Douglas Buckley of Scios Nova (Mountain View, CA).

Chromatography column preparation and characterization. The affinity columns were prepared in the same manner as in Chapter 3. Protein G covalent columns were prepared with anti-insulin C-terminal pentapeptide and anti-GLP-1 7-37. The columns were first tested with insulin (human and bovine) and GLP-1 7-36, respectively, to confirm

binding of whole antigen was occurring. The columns were tested using the same LC setup as in Chapter 3. Oxidized B-chain of bovine insulin was also injected onto the anti-insulin column to check for binding. The antigens were loaded onto the affinity column from loading buffer which was 0.05 M sodium phosphate, 0.05 M potassium sulfate at pH 6.8 or digestion buffer. The bound fragment was desorbed with 0.05 M sodium phosphate, 0.05 M potassium sulfate at pH 3. Characterization of the columns and detection of the desorbed antigen was performed in a manner similar as in Chapter 3, using 210 nm as the wavelength.

Digestion of peptides. Trypsin and α-chymotrypsin at a ratio of 1:8 (w/w) with insulin (human or bovine) and GLP-1 7-36 were dissolved in 0.1 M tricine, 10 mM calcium chloride at pH 7.6 (digestion buffer). Digestion at 37 °C proceeded for 30 min or longer. These conditions were modified slightly from directions from the supplier; tricine buffer was substituted for tris buffer. Before digestion of insulin with clostripain, the clostripain was activated with 2.5 mM DL-dithiothreitol (DTT) for 2 hours at 37°C using the same digestion buffer. The activated clostripain and insulin at a ratio of 1:8 (w/w) were digested at 37°C for 10 min or longer. Pepsin and GLP-1 7-36 at a ratio of 1:8 were dissolved in 0.02 M sodium acetate at pH 3.5 (78). The supplier of pepsin suggests a buffer at pH 2 in order to perform a digestion. The pepsin digestion was stopped by adding 3 M Tris buffer at pH 8.8. The original concentration of insulin and GLP-1 7-36 was 50 μM unless stated otherwise. The digestion processes occurred at 37 °C for 30 min or longer. Trypsin and α-chymotrypsin were used to digest GLP-1 7-36 under the same conditions.

For characterization of the digestion process, the digestions were monitored at half hour to hour intervals by CZE for a total of six hours. Digestion samples were injected onto the CZE system by a 5s, 5kV injection. The CZE capillary was a 80 cm length of 50 μm i.d., 350 o.d. fused silica (Polymicro Technologies, Inc., Phoenix, AZ, USA). The inner surface of the capillary was prepared using the following protocol: 1) rinse capillary with 0.1 M NaOH for 15 min, 2) rinse capillary with H_2O for 5 min, 3) rinse capillary with the migration buffer for 10 min. Migration buffer was 0.1 M tricine at pH 8. The injector to detector distance was 60 cm and the electric field strength was 190 V/cm. Voltage was applied using a Spellman CZE 1000R (Plainview, NY, USA). On-column detection was accomplished using a UV absorbance detector (Spectra 100 from Spectra-Physics, Fremont, CA, USA) at 210 nm.

Epitope mapping. The affinity columns were injected with 20 μL volumes of digested antigen at a flow rate of 10 μL/min. Unbound antigen was collected in a volume of 20 μL. Bound fragments were collected in volumes of 10 μL of desorbing buffer unless stated otherwise. Once the fractions were collected, they were injected onto the CZE system by a 5s, 5kV injection.

Mass spectrometry. Bound peptide fragments were analyzed by MALDI-TOFMS which was performed by the Mass Spectrometry Laboratory in the Chemistry Department at the University of Florida. The instrument used was a Vestec Lasertec benchtop model from PerSeptive Biosystems (Cambridge, MA, USA) with a linear flight tube. 50-100 scans were averaged to produce the mass spectrum for each sample. A Zeos 486 personal computer was used to collect and analyze the data. Data were collected at a rate of 500

MHz. Calibration of the spectra was performed using insulin in a dihydroxybenzoic acid/acetonitrile/trifluoroacetic acid (1%) matrix. The same matrix was used for the peptide fragment samples. The analysis program used was GRAMS 386 from Galactic Industries Corporation (Salem, NH, USA).

Results and Discussion

The first antigen which was used to test epitope mapping using capillary immunochromatography and CZE was insulin. This antigen was chosen because a monoclonal antibody with a linear epitope region containing the terminating five peptides on the B-chain of insulin was available. Three digestive agents were used to digest bovine and human insulin. Trypsin selectively cleaves at the carboxyl side of arginine and lysine. α-Chymotrypsin selectively cleaves at the carboxyl side of tyrosine, tryptophan, phenylalanine and methionine. Clostripain, after activation, will cleave at the carboxyl side of arginine. Figure 4-1 shows the amino acid sequences of human and bovine insulins. The expected peptide fragments from insulin for each enzyme are shown in Figure 4-2.

Anti-Insulin Epitope Characterization

Digestion characterizations. Before epitope mapping was performed, the digestion conditions were characterized. The digestion process was characterized with bovine insulin and trypsin. Figure 4-3 shows electropherograms from the conditions shown in Table 4-1. It was found that the best conditions for digestion followed by CZE was 0.1 M tricine, 10 mM calcium chloride pH 7.6 at 37°C. The best migration buffer for CZE was 0.1 M tricine pH 8. Using tricine buffer for digestion did not appear to have an adverse

Table 4-1. Digestion and CZE Conditions Tested for Insulin Digestion.

Electropherogram in Figure 4-3	1) Digestion Buffer 2) Migration Buffer
A	1) 20 mM Tris-HCl, 10 mM $CaCl_2$ pH 7.74 at 25 °C 2) 0.1M tricine, 0.05 M K_2SO_4 pH 8
B	1) 20 mM Tris-HCl, 10 mM $CaCl_2$ pH 7.74 at 37 °C 2) 0.1M tricine, 0.05 M K_2SO_4 pH 8
C	1) 20 mM Tris-HCl, 10 mM $CaCl_2$ pH 7.74 at 37 °C 2) 0.1 M tricine pH 8
D	1) 0.1 M tricine, 10 mM CaCl2 pH 7.6 at 37°C 2) 0.1 M tricine pH 8

effect on the digestion process.

Bovine insulin digestions by α-chymotrypsin and clostripain were also characterized using the best conditions found with trypsin digested insulin. Figure 4-4 shows electropherograms of A) 50 μM insulin, B) 50 μM insulin digested with clostripain, and C) 50 μM B-chain of insulin. It is clear from the figure that when insulin is digested with clostripain, the B-chain of insulin is not a product. It was of interest to determine the clostripain digestion products of the B-chain of insulin. Figure 4-5 shows electropherograms of A) 50 μM B-chain of insulin, B) a 10 min clostripain digestion of 50 μM B-chain, and C) clostripain and DTT after 25 min. In Figure 4-5 (b), it was not clear whether peak 1 was a digestion product or a byproduct of the reaction. Therefore, clostripain and DTT were allowed to react for 25 min without B-chain of insulin. As is shown in Figure 4-5(c), peak 1 is a byproduct of the reaction and not a digestion product.

However, it was unclear whether the peak shown in Figure 4-4(b) was a result of digestion by clostripain or reduction by DTT. Therefore, an experiment was performed with insulin in the presence of 2.5 mM DTT to determine if the DTT had an effect on insulin. Figure 4-6 shows electropherograms of A) 50 μM insulin, B) 50 μM insulin with DTT after 1 hr 44 min, C) 50 μM insulin with DTT after 5 hr., and D) 50 μM insulin with

DTT after 22 hr. Peak 2 in all electropherograms corresponds to insulin. As is shown in Figure 4-6, the insulin peak remains essentially unchanged even after 22 hrs with DTT. Peak 1, which is due to DTT in solution, increases over time. Therefore, the DTT present during the clostripain digestion has no effect on insulin.

Chromatography column characterization. Before digested insulin could be injected onto the affinity column, whole insulin was tested for binding to the column. In this experiment, 10 μM bovine insulin was dissolved in loading buffer and in digestion buffer. Samples of 20 μL volumes were injected onto a protein G anti-insulin column. This column had 113.7 picomoles of antibody attached, therefore it could theoretically bind 228 picomoles of insulin. Therefore, 10 μM insulin was used because it was just under the maximum binding capability of the column. When insulin was dissolved in loading buffer, the affinity column bound 125 pmol of insulin. When insulin was dissolved in the 0.1M tricine, 10 mM $CaCl_2$, the affinity column bound 117 pmol of insulin. Since there was only a slight decrease in the number of moles of insulin bound with digestion buffer, the digestion buffer could be used to load the digested fractions onto the affinity column. The capacity of the column for insulin was lower than was calculated.

Trypsin digestion. In order to determine if the epitope region of insulin and the monoclonal anti-insulin #C7C9 could be determined by our method, samples from each digestion mixture were injected onto the affinity column. Figure 4-7 shows comparisons of A) normal digestion mixture, B) unbound fragments, C) bound fragments of 48 μM bovine insulin digested with trypsin. It is expected that trypsin would digest insulin into three fragments. There are three major peaks from the digestion process: peaks 1, 3, 5.

Peak 2 shown in all of the electropherograms in Figure 4-7 is a buffer effect and not from the digestion of the insulin. Electropherograms A and B give very similar results, as would be expected since the amount of insulin digested was 5 times the theoretical binding capacity of the column. However, electropherogram C shows that peak 5 bound to the column and nothing else bound.

Chymotrypsin digestion. A comparison of α-chymotrypsin digestions are shown in Figure 4-8. Electropherograms of A) normal digestion mixture, B) unbound fragments, C) bound fragments of 48 μM bovine insulin digested with α-chymotrypsin. It would be expected from a complete digestion of insulin with α-chymotrypsin that seven fragments would be seen. In this case, nine fragments are seen in Figure 4-8(a). In this case, the normal digestion mixture and unbound fragments are again very similar. However, as shown in electropherogram C, there was nothing bound by the affinity column; the peaks which appear in the electropherogram are noise spikes and not peptide fragments, as they are not at a migration time where fragment peaks are shown in the earlier traces. α-Chymotrypsin cleaves insulin at residue 26, which is part of the epitope for the antibody. Therefore, it is expected that there would not be any fragments binding to the affinity column from α-chymotrypsin digestion.

Clostripain digestion. Finally, the clostripain digestions were investigated. Experiments were first performed with 50 μM bovine insulin, but later the concentration was reduced to 10 μM so that the difference between unbound and bound fragments could be observed. Figure 4-9 compares electropherograms of A) normal digestion mixture, B) unbound fragments, C) bound fragments of 10 μM bovine insulin digested with

clostripain. As shown, peak 1 is present in A and B; but it is not present in C. Peak 3 is present in A and C but not in B. Therefore, peak 3 should contain the epitope region of the insulin. MALDI-TOFMS was unable to confirm the presence of the epitope.

Since the epitope for the antibody used was reportedly on the B-chain of insulin, B-chain of bovine insulin was injected onto a C7C9 affinity column to determine if the B-chain was binding. A summary of the experiments performed to determine binding ability are shown in Table 4-2. The B-chain and human insulin were dissolved in loading buffer. As is shown, the B-chain of bovine insulin did not bind as well as human insulin.

Table 4-2: Binding of B-Chain of Insulin

	Flow Rate (μL/min)	Desorbed Peak Area
50 μM B-chain	5	0.301
50 μM human insulin	5	138.55
50 μM B-chain	1	7.139
50 μM human insulin	1	240.5

One explanation for the lack of B-chain binding is that the antibody was specific for human insulin, therefore the epitope region would be changed for bovine insulin by one amino acid. Thus, the next step was to digest human insulin and attempt to bind the fragments. However, when human insulin was digested, bound fragments were similar to the bovine insulin bound fragments. Therefore, a conclusion was reached that the epitope region of this antibody was not linear. The supplier of the antibody was questioned about this discrepancy. It was determined that although the antibody was advertised as having a linear epitope corresponding to the last five amino acids on the B-chain of insulin, this had not been verified by the supplier.

Anti-GLP-1 (7-37) Epitope Characterization

For the second antigen/antibody pair used, GLP-1 7-36 was the antigen and a monoclonal anti-GLP-1 was the antibody. This is a convenient test system since it is well characterized. Studies performed with this antibody have indicated that at least the first three amino acids are contained in the epitope (79). Using immunoprecipitation of α-chymotrypsin digests of GLP-1 7-37 with MALDI-TOFMS, the epitope was narrowed to amino acids 1-13 of GLP-1 7-37 (18). In the present set of experiments, trypsin, α-chymotrypsin and pepsin were used to digest GLP-1 7-36 to produce a "library" of potential epitopes. The expected fragments from these digests are shown in Figure 4-10.

Affinity column binding capacity. Before the determination of the epitope for anti-GLP 7-37 could be performed, an experiment to be certain that GLP-1 7-36 was binding to the affinity column was performed. Therefore, 50 μM GLP-1 7-36 was injected onto the affinity column. The binding capacity of the column for GLP-1 7-36 was determined from a breakthrough curve. The number of moles of GLP-1 7-36 that the column bound was 175 picomoles. Based on the capacity of the protein G column for antibody (10 mg/mL), the theoretical number of moles of GLP-1 7-36 able to bind to the affinity column is 231 picomoles. The results show that although the full theoretical value was not obtained, GLP-1 7-36 was binding to the column in a reasonable manner.

Trypsin digestion. Electropherograms from 50 μM GLP-1 7-36 digested with trypsin for 2 h and 25 min are shown in Figure 4-11. Three electropherograms are shown comparing A) an example of the digest before injection onto the affinity column; B) peptide fragments which did not bind to the affinity column; C) peptide fragments which

bound to the affinity column. There are a total of four peaks shown although only three were expected from the digestion process. From the electrophoresis alone, it is not clear if the extra peak is the result of incomplete digest or contamination with α-chymotrypsin.

Figure 4-11(b) shows that the unbound fraction is virtually unchanged compared to the total digest. It may be expected to observe a loss of the bound peaks in the unbound fraction. However, 1 nmol of the peptides were injected (20 μL of 50 μM) which is well beyond the saturation range of the affinity column. To illustrate loss of peaks, the experiment illustrated in Figure 4-11 was repeated with a lower concentration of GLP-1 7-36 (10 μM). Figure 4-12 shows a comparison of electropherograms for 10 μM GLP-1 7-36 digested with trypsin for 40 min. Peak 2 did not disappear from the unbound sample; however, if the ratios of the areas of peaks 1 and 2 are compared, then it is clear that peak 2 did decrease significantly. In Figure 4-12(a) the ratio is 1.1 and for Figure 4-12(b) the ratio is 1.6.

Figure 4-13 shows a mass spectrum obtained by MALDI-TOFMS from the bound fraction of the trypsin digest of 50 μM GLP-1 7-36. The peak at m/z = 2097.9 corresponds to 1-20 of GLP-1 7-36 and the peak at m/z =1399.8 corresponds to fragment 1-13. Peptide fragment 1-13 is not produced from trypsin; however, it is expected from α-chymotrypsin. The presence of fragment 1-13 in the mass spectrum supports the theory that α-chymotrypsin was present in the trypsin and accounts for the extra peak in the electropherogram of the total digest (Figure 4-11a).

α–Chymotrypsin digestion. Figure 4-14 shows electropherograms from 50 μM GLP-1 7-36 digested with α-chymotrypsin. For this case, if complete digestion had

occurred, five fragments would be expected. However as is shown in Figure 4-14(a), only four fragments are shown suggesting an incomplete digest. From Figure 4-14(b) it appears that peak 4 is binding to the affinity column, as peak 4 is reduced in size relative to peak 3. Likewise, peak 4 is found in the bound fraction shown in Figure 4-14(c). A similar, but more dramatic result is seen when using a lower concentration of the peptide in the digest (10 μM) as shown in Figure 4-15. In this case a similar pattern is observed to Figure 4-14, however peak 4 is completely eliminated in the unbound fraction since the amount injected no longer saturates the column.

MALDI-TOFMS analysis of the bound fraction produced three peaks in contrast to the single peak observed by CZE (Figure 4-15c) as shown in Figure 4-16. The major peak at m/z = 2375.9 corresponds to fragment 1-22. Minor peaks corresponding to fragment 1-20 (m/z = 2100.0) and 1-13 (m/z = 1402.4). Fragment 1-20 is not expected from the α-chymotrypsin digest, but it is a product of trypsin digestion suggesting contamination of the α-chymotrypsin. It is unclear why only one peak was evident in the immunoaffinity bound fraction by CZE instead of the three seen by MALDI-TOFMS. The mass spectrum suggest a dominant peak and relatively minor components. Therefore, perhaps the minor components were not detectable by UV-VIS.

Pepsin digestion. Figure 4-17 shows electropherograms from the pepsin digestion of 50 μM GLP-1 7-36 for 30 min. As is shown in Figure 4-17(a), there are six main fragments as well as numerous smaller peaks. A complete digest is expected to produce five fragments. The presence of extra peaks in the digest again suggests incomplete digest

or contamination with other enzymes. Electrophoretic analysis of the fraction bound to the column shows two peaks binding (Figure 4-17c).

Figure 4-18 shows MALDI-TOFMS spectra of the fraction bound to the affinity column. Again, a more complicated spectrum than that expected from the CZE is seen. Of the peaks in the spectrum, only three are recognizable as GLP-1 7-36 fragments. The unidentified peaks are presumably contaminants. The identifiable peaks are: m/z = 661.5 (fragment 1-6), m/z = 1404.5 (fragment 1-13) and m/z = 1517.7 (fragment 1-14). Fragments 1-6 and 1-14 are expected from pepsin digest. Fragment 1-13 could be from either trypsin or α-chymotrypsin impurities in the pepsin sample. Since fragment 1-6 bound to the affinity column, the number of residues in the epitope region can be narrowed down to 1-6 of GLP-1 7-36.

The fragment 1-6 of GLP-1 7-36 should also be produced by a complete α-chymotrypsin digest and therefore would be expected to be observed in the mass spectrum and CZE of the bound fraction. The lack of this fragment suggests that the α-chymotrypsin digest was incomplete as expected from the electropherogram in Figure 4-12(a).

Concluding Remarks

From the results presented here, it is apparent that immunoaffinity chromatography with CZE and mass spectrometry may have a useful role in epitope mapping. The immunoaffinity column bound only fractions at the N-terminus of the antigen as expected for all of the digests. The pepsin digest produced the smallest identifiable bound fragment, 1-6, thus producing the best defined epitope.

The use of immunoaffinity chromatography in combination with MALDI-TOFMS to analyze enzymatic digests is essentially identical to the use of immunoprecipitation with MALDI-TOFMS reported previously (76). In the present case, we confirm the potential of this approach for determining epitopes and illustrate the use of additional enzymes to define the epitope with higher resolution. The use of CZE as an alternate method for analyzing the bound fraction of the immunoaffinity column is a new addition to the method and provides a number of benefits. CZE can be used as a screening method to determine if an antigen actually contains a linear epitope. This could save the cost of using MS when no linear epitopes are present. Since the method relies on enzyme digests, the use of CZE can also be used to optimize the digest conditions prior to MS analysis. Although not explored in this case, the quantification possible with CZE may allow estimation of the relative affinity of possible epitopes for even finer resolution.

Identification of the peptides bound requires mass spectrometry at present. Since the peptides can only be from a limited number of possibilities, it may be possible to utilize the electrophoretic mobility to identify the peptide fragments (80). Before the method could be completely reliable however, improvements in detection sensitivity would be required so that low level peaks are not missed.

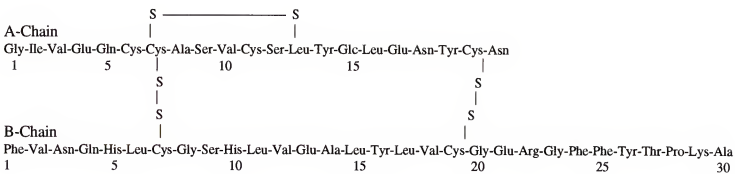

Figure 4-1. The amino acid sequence of bovine insulin. Human insulin substitutions are: A-chain, 8 - Thr; A-chain, 10- Ile; B-chain, 30- Thr.

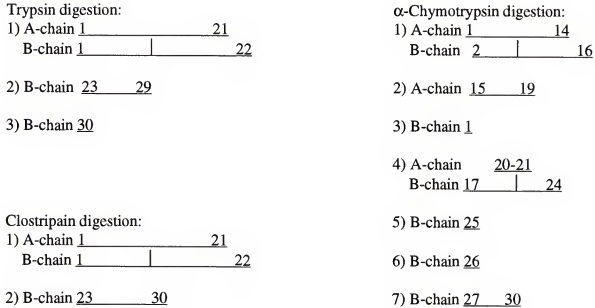

Figure 4-2. Expected digestion fragments from insulin digested with various enzymes.

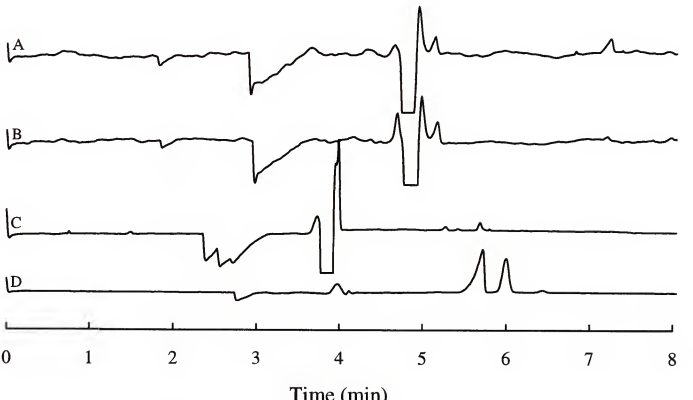

Figure 4-3. Digestion characterization of bovine insulin with trypsin. Electropherograms are for the following conditions: (A) Digestion buffer (DB) is 20 mM Tris-HCl, 10 mM $CaCl_2$ pH 7.74 at 25 °C, migration buffer (MB) is 0.1 M tricine, 0.05 M K_2SO_4 pH 8. (B) DB is 20 mM Tris-HCl, 10 mM $CaCl_2$ pH 7.74 at 37°C, MB is 0.1 M tricine, 0.05 M K_2SO_4 pH 8. (C) DB is 20 mM Tris-HCl, 10 mM $CaCl_2$ pH 7.74 at 37°C, MB is 0.1 M tricine pH 8. (D) DB is 0.1 M tricine, 10 mM $CaCl_2$ pH7.6, MB is 0.1 M tricine pH 8.

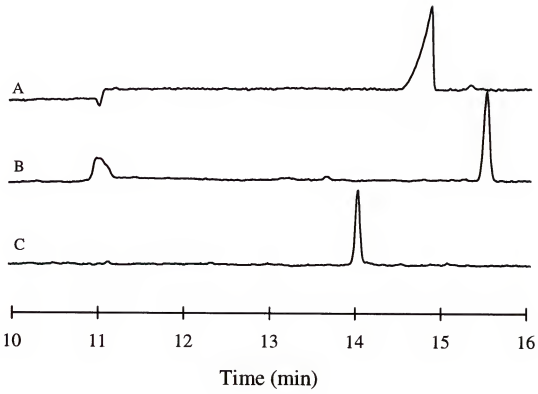

Figure 4-4. A comparison of electropherograms from (A) insulin, (B) clostripain digestion of insulin, (C) B-chain of insulin.

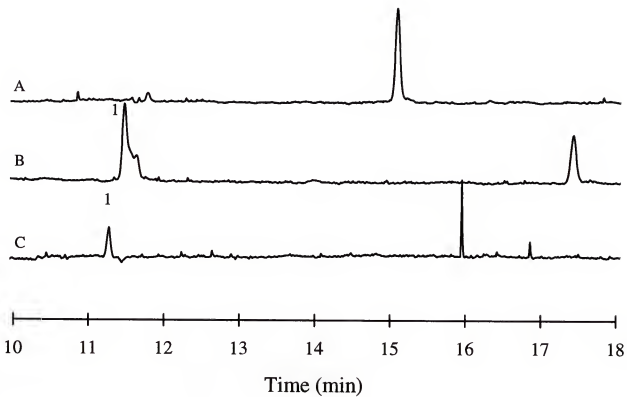

Figure 4-5. Electropherograms of (A) B-chain of insulin, (B) clostripain digestion of B-chain, (C) clostripain with DTT.

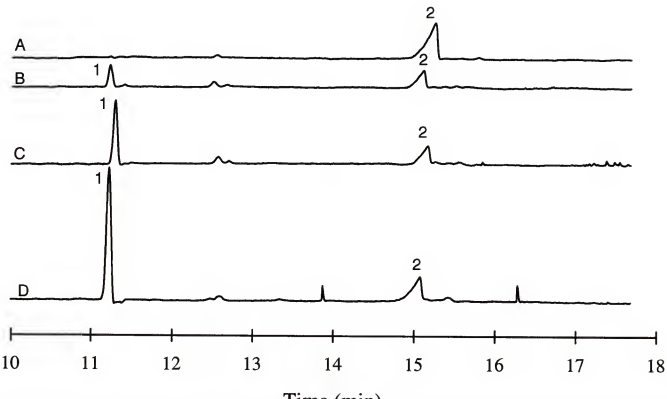

Figure 4-6. Reaction of bovine insulin with DTT. (A) Electropherogram of 50 μM insulin in digestion buffer. (B) Electropherogram of 50 μM insulin with DTT after 1 hr 44 min. (C) Electropherogram of 50 μM insulin with DTT after 5 hr. (D) 50 μM insulin with DTT after 22 hr.

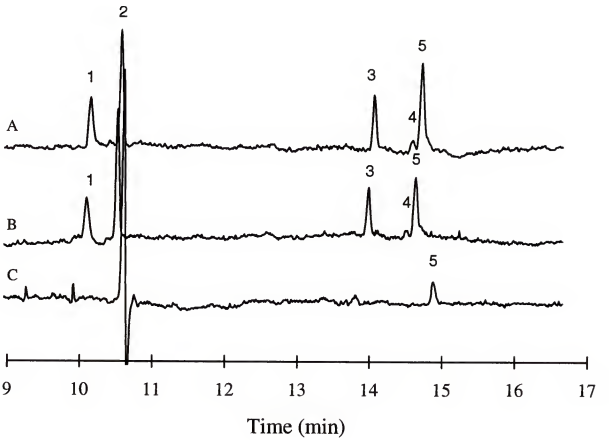

Figure 4-7. Comparison of electropherograms from trypsin digestion of 48 μM bovine insulin. (A) normal digestion, (B) unbound fragments, (C) bound fragments.

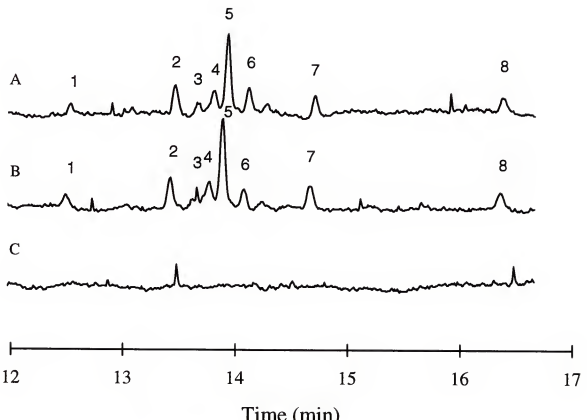

Figure 4-8. Comparison of electropherograms from α-chymotrypsin digestion of 48 μM bovine insulin. (A) normal digestion, (B) unbound fragments, (C) bound fragments.

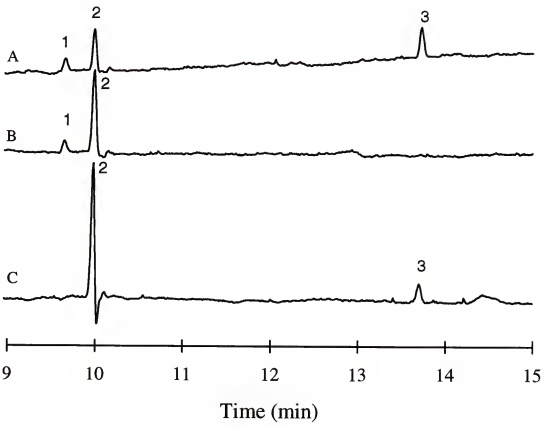

Figure 4-9. Electropherograms showing comparison of clostripain digestion of 10 μM bovine insulin. (A) normal digestion, (B) unbound fragments, (C) bound fragments.

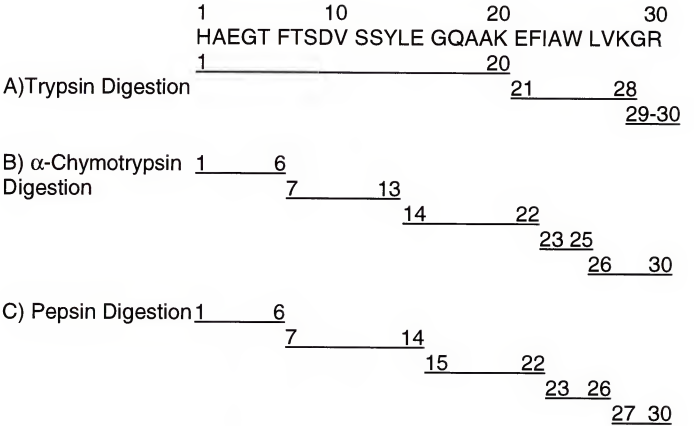

Figure 4-10. GLP-1 amino acid sequence and expected digestion fragments. (A) Three fragments are expected from trypsin. (B) Five fragments are expected from α-chymotrypsin. (C) Five fragments are expected from pepsin.

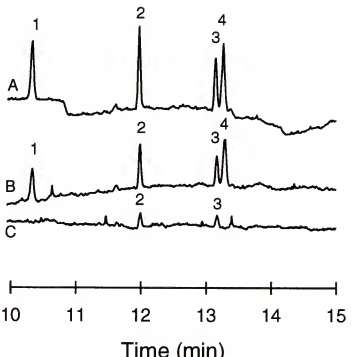

Figure 4-11. Electropherograms showing comparisons of 50 μM GLP-1 7-36 digested with trypsin. (A) normal digestion, (B) peptide fragments which did not bind to the affinity column, (C) peptide fragments which did bind to the affinity column.

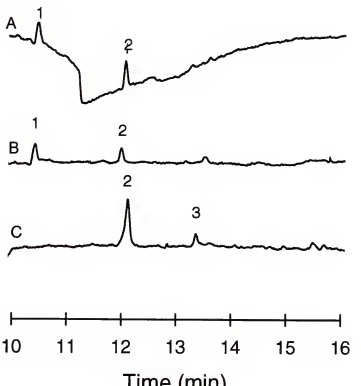

Figure 4-12. Electropherograms of 10 μM GLP-1 7-36 digested with trypsin. (A) normal digest, (B) unbound fragments, (C) bound fragments.

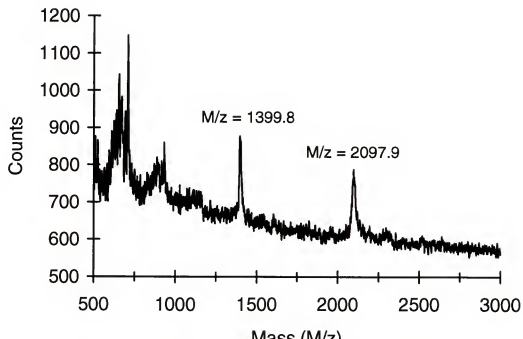

Figure 4-13. Mass spectra of 50 μM bound GLP-1 7-36 fragment. The peak at m/z = 2097.7 corresponds to fragment 1-20 and peak m/z = 1399.8 corresponds to fragment 1-13.

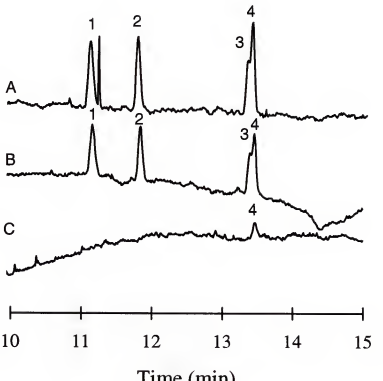

Figure 4-14. Electropherograms of 50 μM GLP-1 7-36 digested with α-chymotrypsin. (A) shows the normal digest, (B) the unbound fragments, and (C) shows the fragments which bound to the affinity column.

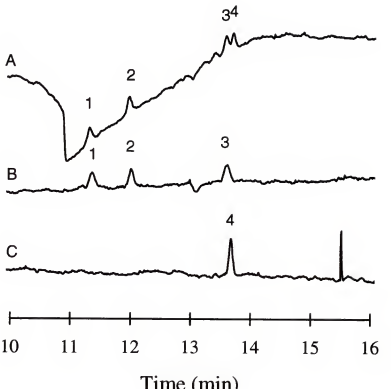

Figure 4-15. Electropherograms of 10 μM GLP-1 7-36 digested with α-chymotrypsin. (A) shows the normal digest, (B) the unbound fragments, and (C) shows the fragments which bound to the affinity column.

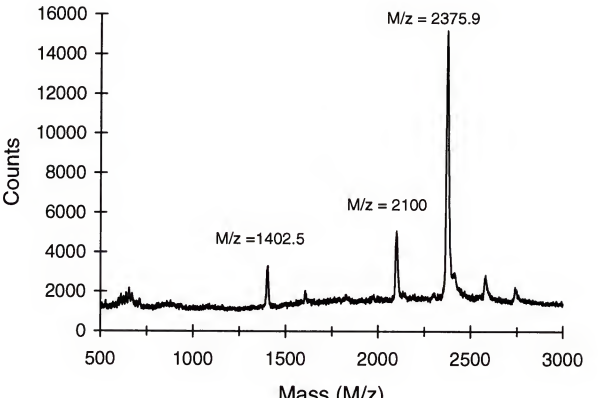

Figure 4-16. Mass spectra obtained from bound fragments of 50 μM GLP-1 7-36 digested with α-chymotrypsin. The major peak at m/z = 2375.9 corresponds to fragment 1-22. Minor peaks are at m/z = 2100.0 (fragment 1-20) and m/z = 1402.4 (fragment 1-13).

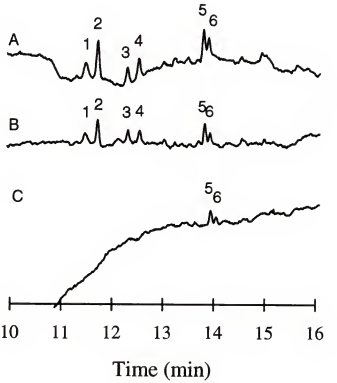

Figure 4-17. Electropherograms from pepsin digest of 50 μM GLP-1 7-36. (A) shows the normal digest, (B) shows the unbound fragments, and (C) shows the bound fragments.

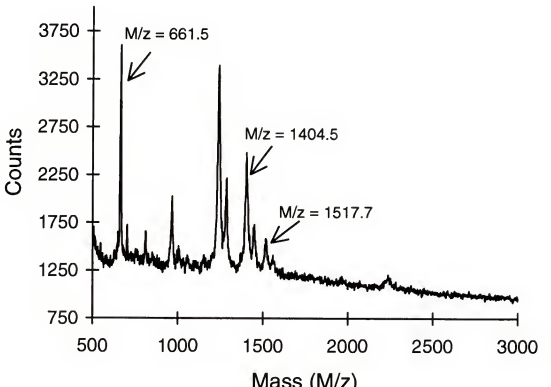

Figure 4-18. Mass spectra from bound fragments of pepsin digest of 50 μM GLP-1 7-36. The peaks identified are: m/z = 661.5 (fragment 1-6), m/z = 1404.5 (fragment 1-13) and m/z = 1517.7 (fragment 1-14).

CHAPTER 5
CONCLUSIONS AND FUTURE WORK

Rapid separations by packed capillary liquid chromatography were obtained. The best results were obtained with 8 μm diameter glass beads packed in 50 μm i.d. fused silica. A high efficiency separation of ascorbic acid was performed in 10.1 s with 666 plates s^{-1}. It was found that not only does column efficiency depend on column i.d. in the range tested, but also on column diameter to particle diameter ratio (ρ). The most important factor for an improvement in column performance was ρ. Perfused particles packed in capillary columns also gave improved results over microbore columns, however the performance of the column was not improved with decreasing ρ or column i.d. as with the pellicular particles. It should be possible to achieve even higher efficiencies by using smaller particles and by decreasing ρ more than was attempted in this dissertation.

A dual column immunoassay using capillary immunoaffinity chromatography can be used to selectively preconcentrate sample for separation by CZE. The best results were obtained using protein G with antibody attached noncovalently. It was possible to use flow rates up to 100 μL/min to load insulin onto an affinity column without loss of sample. Both on-line and off-line experiments were successful. Preconcentration of 25 nM bovine insulin 200-fold was accomplished with a detection limit of 9 nM. The detection limit for insulin by direct injection onto CZE was 2 μM. The long loading times associated with large volume preconcentrations resulted in a loss of insulin.

This system was also used for selective preconcentration of an insulin-spiked bovine serum sample. Direct injection of the insulin-spiked serum sample onto CZE did not allow the insulin zone to be seen; however, after cleanup with an affinity column, this zone was clearly identified. Preconcentration of insulin from serum samples resulted in only 50% of the expected value. This low value indicates that the large number of components in serum may bind non-specifically to the column, thereby limiting the number of open antibody sites for insulin. Improvements for real sample preconcentration will be investigated. By using a different type of LC pump, it may be possible to reduce the desorbing flow rate more than was shown here. With this reduction in flow rate, greater preconcentration effects could be seen. This could decrease the detection limit, perhaps even to picomolar levels.

Another application using immunoaffinity chromatography coupled with CZE was investigated. For this case, immunoaffinity chromatography and CZE in combination with MALDI-TOFMS was explored for linear epitope mapping. From the results presented here, it is apparent that immunoaffinity chromatography with CZE and mass spectrometry may have a useful role in epitope mapping. The immunoaffinity column bound only fractions at the N-terminus of GLP1 7-36 as expected for all of the digests. The pepsin digest produced the smallest identifiable bound fragment, 1-6, thus producing the best defined epitope. From the work performed with insulin and several of its antibodies, it is clear that determining discontinuous epitopes is not feasible using this method. An antibody with an epitope could be tested easily with this system to determine the type of epitope. It is of interest to determine autoantibody antigenic sites since autoantibodies

attack normal cellular components leading to autoimmune diseases such as rheumatoid arthritis. Therefore, autoantibody/autoantigen pairs could be used with the system described here to further elucidate information regarding the epitope region of the autoantibody.

Another possible application using the DCIA system described in this dissertation involves multiple antigen determination. For this case, an antibody which cross-reacts with more than one antigen would be bound to the immunoaffinity column, and the different antigens would be separated by CZE. One possible method for DCIA which has not been explored to a great extent is coupling two capillary chromatography columns. This would prevent the waste of the sample from the first separation technique as seen when a capillary LC column is coupled with CZE.

Another possibility is to couple the immunoaffinity column directly to a mass spectrometer to perform epitope mapping. This would eliminate the CZE separation step; however, the identification process would be faster. During CZE analysis of the bound fragments it was not always possible to see all of the fragments which were later identified with MALDI-TOFMS. Therefore, it would be beneficial to use a more sensitive detector. One detector which could be used is a fluorescence detector. However, the analyte needs to be naturally fluorescent or the analyte needs to be derivatized with a fluorophore before detection.

The dual column system described in this dissertation could also be used for enzyme substrate optimization for enzyme immunoassays. Model substrates are small peptide fragments derived from the physiological target sequences. Affinity chromatography

coupled with CZE could determine substrate specificity for the enzyme. In this case, the enzyme would be attached to the affinity support. A system described recently used reversed phase LC coupled with continuous flow fast atom bombardment mass spectrometry to perform rapid optimization of enzyme substrates (81).

There are many and varied applications for the dual column separation system discussed in this dissertation. A few possibilities were discussed above; however, there are many more applications possible with biotechnology products, such as determining the purity of recombinant proteins. This dual column system could be used to determine purity of recombinant proteins, provided that a known antibody to the protein was available. Thus, there are many potential uses for the dual column system discussed in this dissertation.

APPENDIX A
DERIVATIZATION OF GLASS BEADS

Glass beads of 8 μm diameter were first rinsed with toluene, acetone, methanol and water. The beads were treated with hydrochloric acid as previously described (82). The beads were refluxed for 4 hours with concentrated hydrochloric acid in order to provide a large amount of silanol on the surface of the beads. Water was used to rinse the beads until the pH was neutral, then acteone was used. A vacuum oven at 110°C was used to remove any residual water from the particles.

The silanization of glass particles was adapted from a method described by Hemetsberger *et al.* (83). The hot particles were added to 4 mL of dry toluene and then the reflux flask was purged with dry nitrogen. Chorodimethyloctyldecylsilane was melted and then 200 μL added to the reflux solution. Pyridine was also added at this time. The mixture of chemicals and glass beads were refluxed for 12 hours with stirring.

The particles were washed and centrifuged three times each with the following solvents: benzene, acetone, methanol, methanol:water (1:1), and acetone. The particles were dried at 110°C for 1 hour. Then the particles were added to a solution of dry toluene and trimethychlorosilane. The solution was refluxed for 12 hours with stirring. The particles were washed and centrifuged with the same solvents as previously. The particles were dried in a vacuum oven for 24-48 hrs at 110°C.

APPENDIX B
ELECTRODE PREPARATION

Carbon fiber microelectrodes were prepared by two methods. The first method used previously described techniques (84). A glass capillary (AM systems) containing a single carbon fiber of 9 μm diameter (P-55s from Amoco Performance Products) was pulled to a fine tip with a microelectrode puller (PE-2 Narishige Scientific Instrument Lab, Tokyo, Japan). The fiber was cut after the capillary was pulled, giving 2 electrodes. Using a disposable scapel, the fibers were cut to 0.5 mm long. The carbon fibers were sealed in the capillary by dipping the electrodes in an epoxy (composed of Shell EPON Resin 828 and metaphenylenediamine). Epoxy present on the fiber was removed by dipping only the fiber into hot acetone. The electrodes were left overnight and then heated at 100°C for 2 hours. To make the electrical connection, the electrode was filled with mercury and a platinum wire was inserted.

The second method used capillaries which contained a single carbon fiber. An epoxy available from a hardware store was used to hold the fiber in place. In this case, the epoxy was put on the end of the capillary with a thin wire. These electrodes were left overnight before being used. This method gave electrodes which were not as stable as the first method.

The reference electrode was also prepared in our laboratory. Mercuric chloride and mercury were mixed with a mortar and pestle until the mercuric chloride was saturated

with mercury. Saturated sodium chloride solution was added until a thin paste was made. The paste was placed into capillaries with a semi-closed cracked tip; the capillaries were spun with a centrifuge to make a condensed calomel layer. Mercury and a platinum wire were used to make the electrical connection. The reference electrodes were stored in saturated sodium chloride solution. The new reference electrodes were compared one week after preparation with an electrode made previously which was working well. The two electrodes were placed in a sodium chloride solution and the voltage difference was measured. If the difference was greater than 3 mV the new reference electrode was discarded.

REFERENCES

1) Karlsson, K. E.; Novotny, M. *Anal. Chem.* **1988**, *60*, 1662.

2) Kennedy, R. T.; Jorgenson, J. W. *Anal. Chem.* **1989**, *61*, 1128.

3) Lemmo, A. V.; Jorgenson, J. W. *Anal. Chem.* **1993**, *65*, 1576.

4) Flurer, C. L.; Novotny, M. *Anal. Chem.* **1993**, *65*, 817.

5) Novotny, M. *Anal. Chem.* **1988**, *60*, 500A.

6) Tsuda, T.; Novotny, M. *Anal. Chem.* **1978**, *50*, 271.

7) Unger, K. K.; Lork, K. D.; Wirth, H.-J. in *HPLC of Proteins, Peptides, and Polynucleotides*; ed. M. T. W. Hearn (VCH Publishers, Inc, 1984) Chapter 3.

8) Giesche, H.; Unger, K. K.; Esser, U.; Eray, B.; Trudinger, U.; Kinkel, J. N. *J. Chromatogr.* **1989**, *465*, 39.

9) Unger, K. K.; Jilge, G.; Kinkel, J. N.; Hearn, M. T. W. *J. Chromatogr.* **1986**, *359*, 61.

10) Afeyan, N. B.; Gordon, N. F.; Mazsaroff, I.; Varady, L.; Fulton, S. P.; Yang, Y. B.; Regnier, F. E. *J. Chromatogr.* **1990**, *519*, 1.

11) Cole, L. J.; Schultz, N. M.; Kennedy, R. T. *J. Microcol. Sep.* **1993**, *5*, 433.

12) Giddings, J. C. *Anal. Chem.* **1984**, *56*, 1258A.

13) Bushey, M. M.; Jorgenson, J. W. *Anal. Chem.* **1990**, *62*, 161.

14) Bushey, M. M.; Jorgenson, J. W. *Anal. Chem.* **1990**, *62*, 978.

15) Janis, L. J.; Regnier, F. E. *Anal. Chem.* **1989**, *61*, 1901.

16) Janis, L. J.; Regnier, F. E. *J. Chromatogr.* **1988**, *444*, 1.

17) Janis, L. J.; Grott, A.; Regnier, F. E.; Smith-Gill, S. J. *J. Chromatogr.* **1989**, *476*, 235.

18) Cole, L. J.; Kennedy, R. T. *Electrophoresis*, in press.

19) Cole, L. J.; Kennedy, R. T. *J. Chromatogr.,* submitted for publication.

20) Jorgenson, J. W.; Lukacs, K. D. *Anal. Chem.* **1981**, *53*, 1298.

21) Chu, Y. H.; Avila, L. Z.; Biebuyck, H. A.; Whitesides, G. M. *J. Med. Chem.* **1992**, *35*, 2915.

22) Lauer, H. L.; McManigill, D. *Anal. Chem.* **1986**, *58*, 166.

23) Borra, C.; Han, S. M.; Novotny, M. *J. Chromatogr.* **1987**, *75*, 385.

24) Wilson, W. H.; McNair, H. M.; Maa, Y. F.; Hyver, K. J. *J. High Res. Chrom.* **1990**, *13*, 18.

25) Poole, C. F.; Poole, S. K. *Chromatography Today* (Elsevier Science Publishers, B. V., New York, 1991), Chapter 1.

26) Kennedy, G. J.; Knox, J. H. *J. Chrom. Sci.* **1972**, *10*, 549.

27) Kalghatgi, K.; Horvath, C. *J. Chromatogr.* **1987**, *398*, 335.

28) Fulton, S. P.; Afeyan, N. B.; Gordon, N. F.; Regnier, F. E. *J. Chromatogr.* **1991**, *547*, 452.

29) Gerhardt, G.; Adams, R. N. *Anal. Chem.* **1982**, *54*, 2618.

30) Knox, J. H.; Parcher, J. F. *Anal. Chem.* **1969**, *41*, 1599.

31) Giddings, J. C. *Unified Separation Science* (Wiley, New York, 1991), p. 64.

32) Giddings, J. C. *Dynamics of Chromatography* (Dekker, New York, 1965), Chapter 2.

33) Kaniansky, D.; Marak, J. *J. Chromatogr.* **1990**, *498*, 191.

34) Foret, F.; Sustacek, V.; Bocek, P. *J. Microcol. Sep.* **1990**, *2*, 299.

35) Dolnik, V.; Cobb, K. A.; Novotny, M. *J. Microcol. Sep.* **1990**, *2*, 229.

36) Foret, F.; Szoko, E.; Karger, B. L. *J. Chromatogr.* **1992**, *608*, 3.

37) Foret, F.; Szoko, E.; Karger, B. L. *Electrophoresis* **1993**, *14*, 417.

38) Everaerts, F. M.; Verheggen, T. P. E. M.; Mikkers, F. E. P. *J. Chromatogr.* **1979**, *169*, 21.

39) Kaniansky, D.; Marak, J.; Madajova, V.; Simunicova, E. *J. Chromatogr.* **1993**, *638*, 137.

40) Moring, S. E.; Colburn, J. C.; Grossman, P. D.; Lauer, H. H. *LC-GC* **1990**, *8*, 34.

41) Burgi, D. S.; Chien, R. L. *Anal. Chem.* **1991**, *63*, 2042.

42) Burgi, D. S; Chien, R. L. *Anal. Biochem.* **1992**, *202*, 306.

43) Guzman, N. A.; Trebilock, M. A.; Advis, J. P. *J. Liq. Chromatogr.* **1991**, *14*, 997.

44) Debets, A. J. J.; Mazereeuw, M.; Voogt, W. H.; van Iperen, D. J.; Lingeman, H.; Hupe, K.-H.; Brinkman, U. A. Th. *J. Chromatogr.* **1992**, *608*, 151.

45) Cai, J.; El-Rassi, Z. *J. Liq. Chromatogr.* **1992**, *15*, 1179.

46) Cai, J.; El-Rassi, Z. *J. Liq. Chromatogr.* **1993**, *16*, 2007.

47) Swartz, M. E.; Merion, M. *J. Chromatogr.* **1993**, *632*, 209.

48) Morita, I.; Sawada, J. *J. Chromatogr.* **1993**, *641*, 375.

49) Hoyt, A. M.; Beale, S. C.; Larmann, J. P.; and Jorgenson, J. W. *J. Microcol. Sep.* **1993**, *5*, 325.

50) Harlow, E.; Lane, D. *Antibodies: A Laboratory Manual* (Cold Spring Harbor Laboratory, 1988).

51) Reiss, K. J.; Von Mering, G. O.; Karis, M. A.; Faulmann, E. L.; Lotenber, R.; Boyle, M. D. P. *J. Immunol. Meth.* **1988**, *107*, 273.

52) Horsfall, A. C.; Brown, C. M.; Maini, R. N. *J. Immunol. Meth.* **1987**, *104*, 43.

53) Schroer, J. A.; Bender, T.; Feldman, R. J.; Kim, K. J. *Eur. J. Immunol.* **1983**, *13*, 693-700.

54) Personal communication with Professor Curtis A. Monnig, University of California-Riverside.

55) Lada, M. W.; Schaller, G. M.; Carriger, M. H.; Vickroy, T. W.; Kennedy, R. T. *Anal. Chim. Acta*, in press.

56) Phillips, M.; Queen, W. D.; More, N. S.; Thompson, A. M. *J. Chromatogr.* **1985**, *327*, 213.

57) Afeyan, N. B.; Gordon, N. F.; Regnier, F. E. *Nature* **1992**, *358*, 603.

58) Reiss, K. J.; Von Mering, G. O.; Karis, M. A.; Faulmann, E. L.; Lotenber, R.; Boyle, M. D. P. *J. Immunol.* **1985**, *135*, 2589.

59) Wimalasena, R. L.; Wilson, G. S. *J. Chromatogr.* **1991**, *572*, 85.

60) Riggin, A.; Sportsman, J. R.; Regnier, F. E. *J. Chromatogr.* **1993**, *632*, 37.

61) Riggin, A.; Regnier F. E.; Sportsman, J. R. *Anal. Chem.* **1991**, *63*, 468.

62) de Frutos, M.; Regnier, F. E. *Anal. Chem.* **1993**, *65*, 17A.

63) Chambers, J. C.; Keene, J. D. *Proc. Natl. Acad. Sci. USA*, **1985**, *82*, 2115.

64) Marchaloni, J. J.; Kaymaz, H.; Dedeoglu, F.; Schlutter, S. F.; Yocum, D.E.; Edmundson, A. B. *Proc. Natl. Acad. Sci. USA* **1992**, *89*, 3325.

65) Jiang, W.; Luft, B. J.; Schubach, W.; Dattwyler, R. J.; Gorevic, P. D. *J. Clin. Microbiol.* **1992**, *30*, 1535.

66) Gill, B. M.; Barbosa, J. A.; Hogue-Angeletti, R.; Varki, N.; O'Connor, D. T. *Neuropeptides* **1992**, *21*, 105.

67) Nakajima, K.; Suzuki, K.; Otaki, N.; Kimura, M. *Meth. Enzymol.* **1991**, *205*, 174.

68) Van Regenmortel, M. H. V. *Immunol. Today* **1989**, *10*, 266.

69) Syu, W.-J.; Kahan, L. *Meth. Enzymol.* **1991**, *203*, 295.

70) Geysen, H. M. *Immunol. Today* **1985**, *6*, 364.

71) Geysen, H. M.; Meloen, R. H.; Barteling, S. J. *Proc. Natl. Acad. Sci. USA* **1984**, *81*, 3998.

72) Wang, Z.; Laursen, R. A. *Peptide Research* **1992**, *5*, 275.

73) Scott, J. K.; Smith, G. P. *Science* **1990**, *249*, 386.

74) Moore, W. T.; Wolinsky, J. S.; Suter, M. J.-F.; Farmer, T. B.; Caprioli, R. M. in *Techniques in Protein Chemistry III*, ed. R. H. Angeletti, (Academic Press, San Diego, 1992) p. 183.

75) Suckau, D.; Köhl, J.; Karwath, G.; Schneider, K.; Casaretto, M.; Bitter-Suermann, D.; Przybylski, M. *Proc. Natl. Acad. Sci. USA* **1990**, *87*, 9848.

76) Zhao, Y.; Chait, B. J. *Anal. Chem.* **1994**, *66*, 3723.

77) Dubs, M.-C.; Altschuh, D.; Van Regenmortel, M. H. V. *J. Chromatogr.* **1992**, *597*, 391.

78) Schultz, N. M. PhD. Dissertation, Dec. 1994, University of Florida, Gainesville, FL.

79) Personal communication from Dr. Douglas Buckley, Scios Nova, Mountain View, CA.

80) Cifuentes, A.; Poppe, H. *J. Chromatogr. A* **1994**, *680*, 321.

81) Berman, J.; Green, M.; Sugg, E.; Anderegg, R.; Millington, D. S.; Norwood, D. L.; McGeehan, J.; Wiseman, J. *J. Biol. Chem.* **1992**, *267*, 1434.

82) Aue, W. A.; Hastings, C. R. *J. Chromatogr.* **1969**, *42*, 319.

83) Hemetsberger, H.; Kellerman, M.; Ricken, H. *Chromatographia* **1977**, *10*, 726.

84) Kelly, R. S.; Wightman, R.M. *Anal. Chim. Acta* **1986**, *187*, 79.

BIOGRAPHICAL SKETCH

Laura J. Cole was born in Ann Arbor, Michigan, on July 17, 1968. She received a Bachelor of Arts degree with majors in biology and chemistry from Albion College in May 1990. She decided to combine both of these interests and pursue a graduate degree in the area of bioanalytical chemistry. Just two weeks after her marriage in August of 1990, she moved to Gainesville to study with Dr. Robert T. Kennedy at the University of Florida. She completed her research and obtained her Doctorate of Philosophy degree in May of 1995.

I certify that I have read this study and that in my opinion it conforms to acceptable standards of scholarly presentation and is fully adequate, in scope and quality, as a dissertation for the degree of Doctor of Philosophy.

Robert T. Kennedy, Chairman
Assistant Professor of Chemistry

I certify that I have read this study and that in my opinion it conforms to acceptable standards of scholarly presentation and is fully adequate, in scope and quality, as a dissertation for the degree of Doctor of Philosophy.

Roger L. Bertholf
Associate Professor of Pathology
and Laboratory Medicine

I certify that I have read this study and that in my opinion it conforms to acceptable standards of scholarly presentation and is fully adequate, in scope and quality, as a dissertation for the degree of Doctor of Philosophy.

Nigel G. Richards
Assistant Professor of Chemistry

I certify that I have read this study and that in my opinion it conforms to acceptable standards of scholarly presentation and is fully adequate, in scope and quality, as a dissertation for the degree of Doctor of Philosophy.

Daniel R. Talham
Assistant Professor of Chemistry

I certify that I have read this study and that in my opinion it conforms to acceptable standards of scholarly presentation and is fully adequate, in scope and quality, as a dissertation for the degree of Doctor of Philosophy.

James D. Winefordner
Graduate Research Professor of
Chemistry

This dissertation was submitted to the Graduate Faculty of the Department of Chemistry in the College of Liberal Arts and Sciences and to the Graduate School and was accepted as partial fulfillment of the requirements for the degree of Doctor of Philosophy.

May 1995

Dean, Graduate School